Plasma-derived exosomes as potential biomarkers for pediatric acute leukemia.

by

Eva Sørensen

Master thesis

60 credits

Department of Bioscience

Faculty of Mathematics and Natural Sciences

UNIVERSITY OF OSLO

July 2020

Plasma-derived exosomes as potential biomarkers for pediatric acute leukemia

http://www.duo.uio.no/

Print: Reprosentralen, Universitetet i Oslo

ACKNOWLEDGEMENTS

This study was performed at the department of pharmacology at Rikshospitalet, Oslo University Hospital.

A special thanks to my supervisor Marit Inngjerdingen for giving me the opportunity to be a part of this project. Your guidance and council have been indispensable. Thank you for your patience and trust.

Thank you to all the members of the innate lymphocyte group (Inngjerdingen group) for creating a good learning environment and workspace. I appreciate all your constructive feedback throughout this process, always making me better.

A huge thank you to my parents who have helped me both mentally and financially through this time. Without you I would not be where I am today.

ABSTRACT

The purpose of this study was to find whether exosomes can function as biomarkers for acute leukemia in children, with the long-term goal to assess whether exosomes can be used to predict risk of relapse. Exosomes are small, extracellular vesicles released by different cell types, and are present in all body fluids. Exosomes are responsible for a multitude of physiological functions by their ability to transfer molecular information and reprogram target cells. Exosomes are reported to mimic their parental cell, which implies the possibility to identify the cellular origins of exosomes isolated from body fluids. Cancer cells are found to be avid exosome producers, several studies show that cancer patients have higher amounts of exosomes in blood or urine compared to healthy controls. Adult acute myeloid leukemia patients have been found to have an increased exosomal load in blood plasma, and we therefore hypothesized that plasma from pediatric acute leukemia patients at diagnosis may be enriched with cancer-spesific exosomes. We confirmed successful isolation of exosomes from blood plasma, and we discovered a tendency for the exosomal marker CD63 being a negative marker for B-cell derived exosomes in ALL patients at diagnosis. Further, our data suggest an increase in extracellular vesicle content for the ALL patients compared to the healthy controls. When screening for potential protein signatures originating from exosome isolates from one patient, we found 9 potential biomarkers which should be further analyzed. A future goal would be to develop methods to assess an exosomal profile in plasma of pediatric acute leukemia patients as a sensitive, non-invasive monitoring of disease progression and risk assessment.

TABLE OF CONTENTS

ACKNOWLEDGEMENTS IV

ABSTRACT VI

TABLE OF CONTENTS VIII

1 INTRODUCTION 1

1.1 ACUTE LEUKEMIA 1

1.1.1 TREATMENT OF PEDIATRIC LEUKEMIA 2

1.2 EXTRACELLULAR VESICLES AND EXOSOMES 3

1.2.1 EXOSOME BIOGENESIS 4

1.2.2 EXOSOME COMPOSITION 5

1.2.3 UPTAKE AND COMMUNICATION PATHWAYS 6

1.2.4 EXOSOMES AS BIOMARKERS IN CANCER 7

1.3 IDENTIFYING ACUTE LEUKEMIA-DERIVED EXOSOMES 8

1.3.1 EXOSOMAL MARKERS 8

1.3.1 ACUTE LEUKEMIA MARKERS 9

1.4 ISOLATION AND CHARACTERIZATION OF EXOSOMES FROM PLASMA 10

1.4.1 COMMON ISOLATION METHODS 10

1.4.2 APPROACHES FOR EXOSOME CHARACTERIZATION 11

2 AIM OF THE STUDY 12

3 MATERIALS AND METHODS 13

3.1 CLINICAL SAMPLES 13

3.2 EXOSOME ENRICHMENT USING SIZE-EXCLUSION CHROMATOGRAPHY. 14

3.3 SAMPLE PREPARATION FOR IMAGESTREAM 16

3.4 EXOSOME ENRICHMENT USING EXOSOME PURIFICATION KIT 18

3.5 NANOPARTICLE TRACKING ANALYSIS 20

3.6 ELECTRON MICROSCOPY 21

3.7 EXOCET QUANTITATION ASSAY 21

3.8 BCA PROTEIN ASSAY 23

3.9 SDS-PAGE AND WESTERN BLOTTING 24

3.10 ANTIBODY ARRAY ANALYSIS 27

3.11 STATISTICAL ANALYSIS 31

4 RESULTS 32

4.1 CHARACTERIZATION OF SMALL EVS IN PLASMA OF ACUTE LEUKEMIA PATIENTS 32

4.1.1 SMALL EV DETECTION USING IMAGESTREAM TECHNOLOGY 32

4.1.2 Small EV detection using conventional methodology *33*
4.2 Quantifying exosomes in patients at diagnosis and during treatment *37*
4.3 Screening for EV biomarkers *41*
5 Discussion **45**
5.1 Methodological considerations *45*
5.1.1 Patient samples 45
5.1.2 Exosome isolation 45
5.1.3 ImageStream subset specific analysis 47
5.1.4 Measuring exosomal concentration 48
5.1.5 Biomarker assay 49
5.2 Findings *50*
5.2.1 Characterization of small EVs in pediatric patients 50
5.2.2 Quantification of exosomes 52
5.2.3 Screening for biomarkers in BCP-ALL 54
5.3 Conclusion *57*
5.4 Future perspectives *57*
References **60**
Appendix 1: Abbreviations **64**
Appendix 2: Patients and controls **66**
Appendix 3: Buffers and solutions **67**
Appendix 4: Antibodies **70**

1 INTRODUCTION

1.1 ACUTE LEUKEMIA

Leukemia is a malignant disease that arises from hematopoietic stem cells in the bone marrow and is classified by how quickly the disease develops and by the different hematopoietic stems cells that are affected (1). The disease development is either acute or chronic, meaning acute leukemia cells multiply at a faster rate than the chronic leukemia cells. In both cases, the abnormal blood cells will accumulate in the marrow, spread to the blood and other tissues, and result in decreased production of healthy blood cells. The malignancy affects the different stages of hematopoiesis in either the lymphoid or the myeloid arms, and the disease is thereby characterized as either lymphocytic leukemia or myeloid leukemia (1). Figure 1.1 illustrates the different stages of myeloid and lymphoid hematopoiesis, and where the different malignancies can develop.

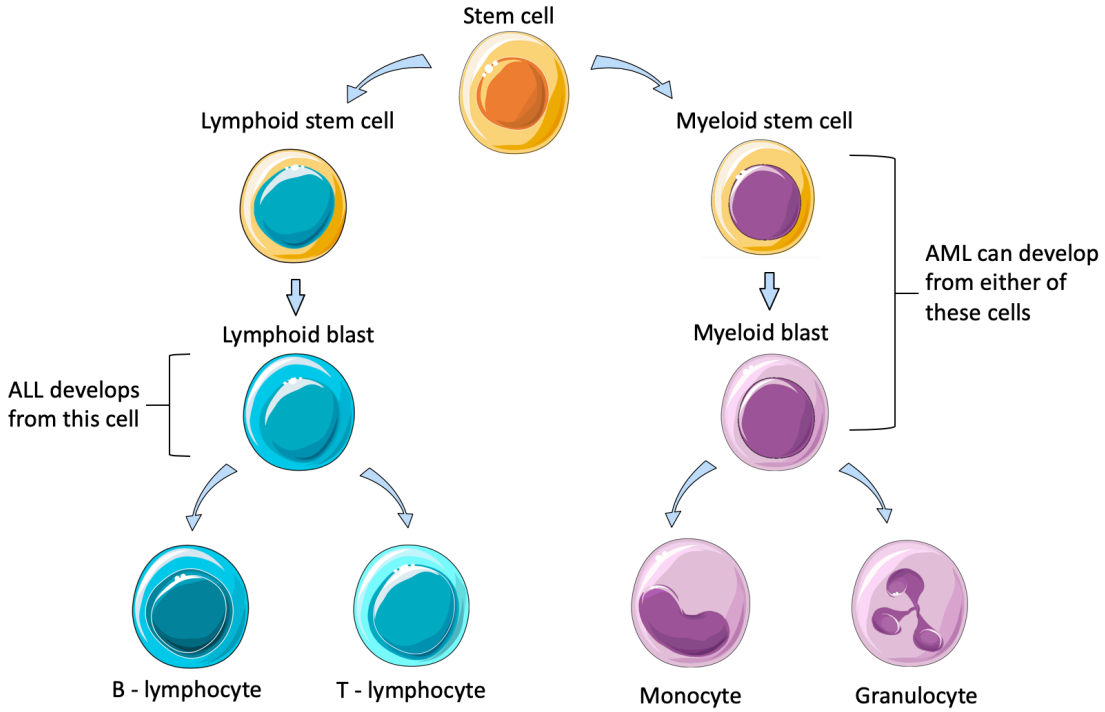

Figure 1.1 Schematic illustration of the main steps of lymphoid and myeloid hematopoiesis. The developmental origins of malignancies and the relationship of the cellular subtypes of leukemia is depicted.

This gives us four main groups of leukemic cancers: Chronic myeloblastic leukemia (CML), acute myeloblastic leukemia (AML), chronic lymphoblastic leukemia (CLL), and acute

lymphoblastic leukemia (ALL). These diseases all encompass different sub-types depending on their origin and molecular composition. In this thesis we will focus on childhood acute leukemia, both ALL and AML. AML is a very heterogenous disease with multiple sub-types, but we have treated this as one group in this thesis. Pediatric ALL is further divided into two main sub-types, either B-cell precursor (BCP-ALL) or T-cell derived (T-ALL) which is mainly treated as one group in this thesis due to limited access to samples (1).

Acute leukemia accounts for over a third of all pediatric cancers, making leukemic cancer the most common malignant disease in children (2). AML makes up approximately 15% of these cases (3), while ALL consists of the remaining 85% , with a prevalence peak between the ages of 2-5 years (4, 5). More than 80 % of the ALL cases are BCP-ALL, while the remaining are T-ALL (1).

1.1.1 TREATMENT OF PEDIATRIC LEUKEMIA

Diagnosis and classification of both AML and ALL are based on cellular morphology, phenotype, cytogenetics and molecular genetics. At diagnosis the patients are divided into risk groups based on age and white blood cell (WBC) count, from standard risk (SR), intermediate risk (IR) to high risk (HR). The backbone of treatment is chemotherapy according to common Nordic protocols (NOPHO), and varies depending on the immunophenotypic and cytogenetic factors (6).

For ALL, the treatment protocol is divided into a remission-induction phase (79 days), consolidation therapy phase, and a maintenance phase, with a total of 2.5 years in treatment (6). For some high-risk patients or those with resistant disease, chemotherapy is combined with stem cell transplantation (SCT) or immunotherapy. In ALL, the treatments are most effective for BCP-ALL, with a 5-year overall survival above 90% (7). The prospects for T-ALL patients are poorer, and all T-ALL patients are categorized as high-risk patients.

AML is more challenging to treat, as it is very heterogeneous and comes in many different sub-types (8, 9). However, new treatments have changed the disease from a fatal to a possibly curable disease. Treatment consists of a remission-induction phase with 2-3 rounds of chemotherapy, followed by central nervous system (CNS) prophylaxis and intrathecal chemotherapy ending with consolidation therapy. The treatment is for 6 months and is quite demanding on the patients, risking severe toxicity and death. The patients with high risk,

resistance or relapse, are given a stem cell transplantation (8, 9). Unfortunately, because of the heterogeneity of the disease it is normal for AML blasts to be resistant to conventional therapies, and even though the current treatments lead to an overall survival of 70%, about 30-40% of the AML patients will relapse (8, 9). This highlights the need for improvement of early detection of malignant cells, and for early prediction of relapse risk (1).

The current protocol for measuring treatment response for both ALL and AML is through repeated bone marrow aspirates to detect minimal residual disease (MRD) (10). MRD is a measure of remaining cancerous cells, and if the patient is in remission, it can be as little as one malignant cell amongst a million healthy. This submicroscopic disease, if left undetected, eventually leads to relapse when the remaining leukemic cell(s) regrow (11). It is therefore important to establish a reliable, preferably less invasive method of MRD detection and monitoring.

Both benign and malignant cells can release numerous exosomal vesicles into the peripheral circulation as a means of communication with their surroundings. Together with the fact that exosomes are said to mimic their parental cell, this introduces the possibility of detecting either residual leukemic cells through exosomal identification, or to exploit exosomes as biomarkers for relapse risk. Accurate identification of leukemic exosomes in patient plasma may therefore have the potential to become a less invasive method of monitoring disease progression.

1.2 EXTRACELLULAR VESICLES AND EXOSOMES

All cells, normal and cancerous, are able to discharge different lipid-enclosed vesicles into the extracellular environment in response to external and internal stimuli (12). These extracellular vesicles (EVs) are transferred between cells, allowing exchange of information and mediating intercellular communication (12, 13).

EVs show considerable heterogeneity with distinctly different intracellular origin, size and functional properties (14, 15). They are classically divided into three different subtypes depending on their biogenesis and size. Apoptotic bodies are larger vesicles (500-2000 nm) blebbing from cells undergoing apoptosis. Microvesicles (MVs) (100-1000 nm), also termed ectosomes or microparticles, are shed directly from the plasma membrane (PM) (16). Exosomes, defined by their small size (40-150 nm), originate from intraluminal vesicles (ILV)

being released from the endosomal pathway (17, 18). Figure 1.2 shows how the various types of EVs are generated.

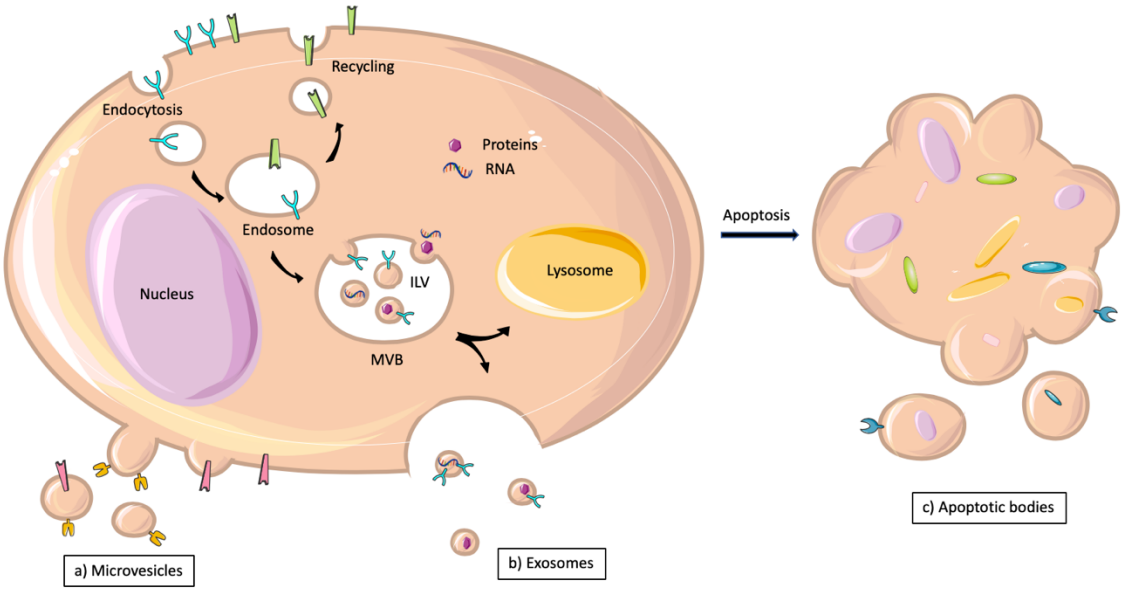

Figure 1.2 Illustration of the formation and release of the different subtypes of EVs. a) Microvesicles are produced by outward budding and shedding directly from the plasma membrane. b) Exosomes are generated within multivesicular bodies (MVBs) of the endosomal pathway, by inward budding, and are released when the MVB fuse with the plasma membrane. c) Apoptotic bodies are released by membrane blebbing from cells undergoing apoptosis.

Exosomes have been detected in various body fluids including urine, blood, breast milk, and saliva (14, 19). While initially thought to represent vessels for cellular waste elimination, exosomes are now recognized as important components in a number of physiological and pathological processes (20, 21). These membrane-enclosed vesicles contain lipids, proteins and nucleic acids which they can exchange with target cells as means of intercellular communication able to alter and even reprogram the recipient cell (15, 19).

1.2.1 EXOSOME BIOGENESIS

In contrast to the larger EVs, exosome biogenesis originates from the endosomal network (13, 22). Figure 1.2 illustrates how the different subtypes of EVs are formed as well as a detailed representation of exosomal biogenesis. Exosome formation begins with the inward budding of the late endosome, creating intraluminal vesicles (ILVs) in the endosomal compartment (15). These compartments are called multivesicular bodies (MVB) and are either routed for degradation, recycling, or exocytosis (23). The MVBs destined for exosome generation will fuse with the plasma membrane and release their ILVs into the extracellular environment (15,

20). Once secreted, the ILVs are termed exosomes. Three different complexes have been identified to mediate this process of biogenesis; the endosomal sorting complex required for transport (ESCRT), tetraspanin protein complexes and ceramide complexes. These components are thought to work independently from each other and regulate the routing and sorting of spesific exosomal cargo, probably generating different types of exosomes (22). In this thesis, whenever exosomes are mentioned, we are talking about small EVs with endosomal origins.

1.2.2 EXOSOME COMPOSITION

Exosomes can be further defined by their selectively loaded cargo which is characteristic to their endosomal biogenesis (13, 22). Because of the double inward budding, first from the PM and then the endosomal membrane, the exosome surface contains receptors, transmembrane proteins and lipids largely mirroring that of the plasma membrane of the parental cell (13, 22). The lipid bilayer is rich in phospholipids, cholesterol and sphingolipids as well as surface proteins such as adhesion molecules, antigen presenting proteins (MHC class I and II), and tetraspanins (20, 22). The basic structure of an exosome is shown in figure 1.3.

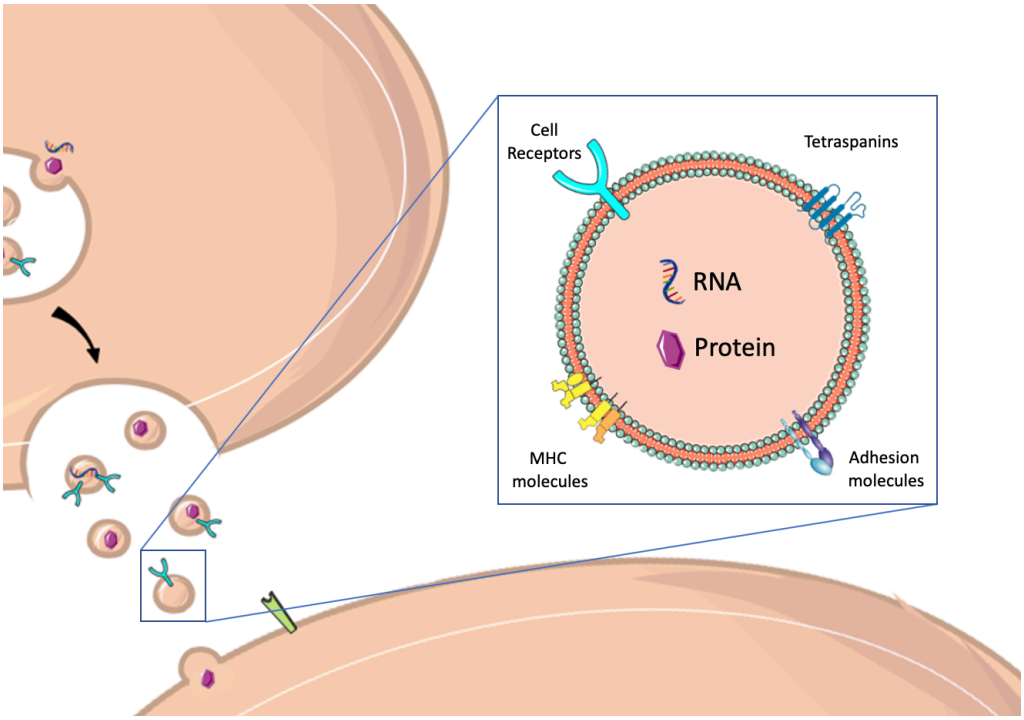

Figure 1.3: Schematic representation of an enlarged exosome composed of a lipid bilayer containing transmembrane proteins and enclosing soluble proteins and RNA (24).

The tetraspanin membrane proteins are assembled into microdomains during the formation of intralumenal vesicles in the MVB biogenesis and are therefore consequently enriched in various EV subtypes, including exosomes (22). The tetraspanins are comprised of a superfamily of > 30 proteins, all sharing a common four-transmembrane domain (12). Some tetraspanins are restricted to a distinct tissue, like CD37 and CD53 belonging to hematopoietic cells, while others like CD81, CD63, and CD9 are found in most cells (16). The tetraspanin microdomains are also thought to help the routing and sorting of vesicle cargo as well as binding and uptake to target cells (13, 16, 25). Recent observations indicate that the tetraspanin content varies according to the different functional properties of the exosomes (13). This is discussed in more detail below.

Besides the membrane-bound proteins, the exosomes are internally loaded with molecules designated for horizontal transfer to recipient cells (22). Within the exosomal lumen we find either noncoding RNA (such as microRNA), mRNA, and non-membrane proteins that can dictate the functional properties of the vesicles (23). RNA transcripts, for instance, have been found to be enriched up to 100 fold in exosomes compared to the donor cell (17). This type of transcript transfer can lead to gene regulation either by miRNA or translation of mRNA in the receiving cell (16, 23).

1.2.3 UPTAKE AND COMMUNICATION PATHWAYS

As the exosomes originate from the plasma- and endosomal- membrane they contain information linked to the parental cells extracellular and intracellular environment (23). This molecular message can selectively be taken up by proximal or distantly located cells as the released exosomes navigate through body fluids (16).

The precise mechanisms directing the exosomes to specifically target one cell over another remains in the early stages of comprehension (12). However, once they arrive at the pre-designated target cell, the cargo is received either through internalization or surface receptor activation (20, 22). The latter means the exosome surface receptors can bind and directly activate downstream signaling pathways in the responding cell (26). Alternatively, the exosomes can be internalized and discharge their content into the target cell where they deliver functional proteins or RNA (12). In both cases the exosomes are able to transmit their

information to a receiving cell and alter its function and/or phenotype (20, 22). The exosomal uptake and communication pathways are depicted in figure 1.4.

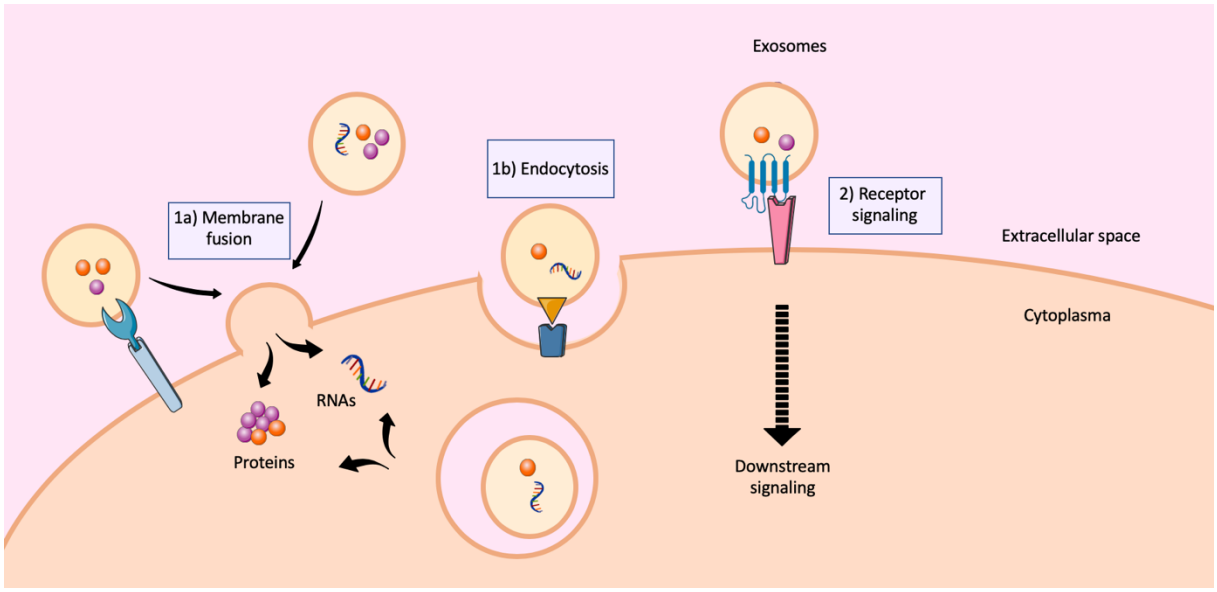

Figure 1.4: Schematic representation of exosomal uptake and communication pathways. When exosomes dock on their target cell their molecular information is transmitted through two different mechanisms. 1) Internalization of the exosome by either a) membrane fusion or b) endocytosis; both releasing their active molecules into the cytosol for further processing. 2) Establishing surface receptor-ligand binding and activating specific pathways that impact the fate of the recipient cell.

1.2.4 EXOSOMES AS BIOMARKERS IN CANCER

Intercellular communication via exosomes in the circulation is mediated by their characteristic extracellular receptors and cargo. Therefore, the possibility of using exosomes as biomarkers has prompted an ample amount of studies in various diseases, particularly in cancer (22, 24). This rapidly expanding research field has elevated our understanding of tumorgenesis, reporting that exosomes derived from cancer cells provoke biological effects that enhance tumor progression, suppress immune responses and even cause treatment resistance (19, 21).

Exosomes are shown to contain cancer-specific components such as oncoproteins and microRNA (miRNA) originating from the tumor host cell (19, 21). Coupled with the fact that exosomes are accessible from almost all body fluids this has made exosomes attractive surrogates for early detection of cancer (19, 21).

Tumor cells are found to be avid exosome producers, showing elevated amounts of tumor-derived exosomes in plasma of cancer patients (22). An increased exosomal load has been identified in plasma of newly diagnosed adult AML patients, and found to correlate with a higher risk of relapse (27). In contrast, patients in complete remission are shown to have low exosomal levels comparable to that of healthy controls (27).

Based on these observations we hypothesize that pediatric acute leukemia patients may have the same elevated exosomal plasma levels, and/or have exosomes enriched with cancer spesific proteins not found in exosomes derived from healthy controls. We therefore consider the potential for exosomes to function as biomarkers for early detection of cancer recurrence by quantifying and identifying an exosomal profile from plasma of pediatric acute leukemia patients.

1.3 IDENTIFYING ACUTE LEUKEMIA-DERIVED EXOSOMES

Since exosomes are thought to mimic their originating cell, acute leukemia-derived exosomes are expected to carry myeloid or lymphoid markers. Consequently, one should be able to classify subsets of exosomes originating from acute leukemia by combining exosome- and leukemia-specific markers.

1.3.1 EXOSOMAL MARKERS

Exosomes are found to have a conserved set of tetraspanin surface markers that are common for all cell types, due to the tetraspanins' important role in exosome biogenesis (17, 22). CD63, CD9 and CD81 are enriched in late MVBs, and for this reason they are widely used as exosomal biomarkers (13, 15). However, several studies have shown that this criterion on its own is not always sufficient to discriminate exosomes from other PM-derived vesicles. For instance, CD9 has been found in larger vesicles not associated with the endocytic pathway, and both CD63 and CD81 have been detected in microvesicles (13, 16). Furthermore, recent evidence suggests that the tetraspanin content is to some extent cell-type dependent (19). These variations in tetraspanin content must be taken into consideration when generating an expression profile for acute leukemia-derived exosomes.

1.3.1 ACUTE LEUKEMIA MARKERS

Acute leukemia is a diverse group of malignancies with various lineage spesific surface markers. Both within AML and ALL there is a clonal heterogeneity resulting in lack of defined target antigens and one single marker will not be enough to define an entire population. For this reason, identification of leukemia cell subsets often requires a combination of several surface markers.

Classical phenotypic markers that are used to define BCP-ALL leukemia include CD19 and CD20, CD10, and cytosolic CD79a. For the T-ALL, surface markers that are most commonly used for detecting blasts are CD3 (both surface and cytosolic), CD4, CD7, and CD1a (11). None of the listed markers are necessarily cancer specific.

For AML, a combination of several myeloid (CD13, CD15, CD33, and CD117), and monocytic markers (CD11b/c, CD14, and CD64) are used. Also, in AML, the hematopoietic stem cell marker CD34 is particularly upregulated compared to lymphoid leukemias.

In this thesis we decided to use tetraspanins CD63 and CD81 as exosomal markers, since they are most frequently used in exosomal identification (28). However, as mentioned, several studies have shown that these tetraspanins are not always sufficient to discriminate between exosomes and other EVs (16). To further distinguish between normal cell-derived and leukemic-derived exosomes we wanted to identify the presence of leukemic-associated antigens (LAA) on the small EVs. In this case we stained with a haemopoietic stem cells marker, CD34, and a B-lymphocyte marker, CD19.

A possible drawback with this method is exosomal heterogeneity. The fact that acute leukemia consists of a multitude of subtypes, each with its own molecular profile, classifying exosomes based on parental-cell markers represents a special challenge. There is also no way of knowing if the exosomes testing positive for the exosomal markers (CD63 and CD81) are the same exosomes testing positive for the leukocyte markers.

1.4 ISOLATION AND CHARACTERIZATION OF EXOSOMES FROM PLASMA

Due to the increasing interest in characterization and classification of the different sub-populations of secreted vesicles, there has been a large methodological diversity in techniques used for specific isolation and analysis of bona-fide exosomes (12, 15). Purification of exosomes from other small EVS is difficult, and the currently used protocols only discriminate between small and large EVs (15, 20).

1.4.1 COMMON ISOLATION METHODS

Exosomes are classically enriched by sequential centrifugation to remove cells and larger EVs, where the smallest vesicles are collected by high speed ultracentrifugation. This procedure cannot, however, separate the different subsets of small EVs from each other (19, 29). Ultracentrifugation is therefore often combined with sucrose density gradients, which can for example separate small EVs from other small particles (19, 29). Ultracentrifugation is time-consuming, tedious, and is also associated to rupture of the vesicles and thus potential loss of functional activity.

Recently, more convenient and commercially developed procedures have become available for exosome enrichment. The isolation kits are based on different principles including affinity purification, precipitation, and gel filtration (30). However, the different kits are shown to yield inconsistent amounts of exosomes, size distributions and different intensity signals for exosomal markers during immunoblotting (30).

While these methods may allow separations of small extracellular vesicles (sEV) from larger EVs, separating sEVs from other contaminants in plasma greatly challenges the isolation (31). Not only does plasma contain larger vesicles like microvesicles and apoptotic bodies, but also proteins and lipoproteins that can be co-isolated when using centrifugation protocols (31). This co-isolation is due to the aggregation of proteins when spun at high velocities, and the lipoproteins having a similar size and density as the exosomes (31). To lower the complexity of the plasma sample, size-exclusion chromatography (SEC) has been introduced as an approach to enrich for exosomes (31). With this technique, the abundancy of contaminating plasma proteins such as albumin is also greatly reduced.

1.4.2 APPROACHES FOR EXOSOME CHARACTERIZATION

Different methods are used for characterization of exosomes. For phenotypic analysis of protein content, commonly used methods include flow cytometry or western blotting (32). Multiparameter flow cytometry can be utilized to analyze exosomes captured on beads, using labeled antibodies and can be used to assess exosomal surface markers (20, 33). Unfortunately, single exosomes cannot be analyzed by flow cytometry as current flow cytometers cannot reliably detect objects below 500 nm, which is way above the size-range of exosomes which is between 40 - 150 nm (14). To surpass this limitation, the image platform ImageStream^{x}, which combines the speed and sensitivity features of flow cytometry with the detailed imagery of fluorescence microscopy can be utilized. The ImageStream can detect particles down to 50-100 nm in size which will allow detection of small EVs (13, 34).

2 AIM OF THE STUDY

The aim of this thesis was to assess whether exosome load is increased in children with acute leukemia with the long-term goal to assess whether exosomes has prognostic value as biomarkers for early prediction of leukemic relapse in children with acute leukemia. The objective was to identify exosomes specific for leukemia and quantify the presence of exosomes in plasma of patients versus healthy controls. Using these vesicles as biomarkers in a liquid biopsy is beneficial not only by being a less invasive method compared to bone marrow aspirations but could also give the possibility for more frequent monitoring of relapse.

Specific aims set for this thesis:

- Identify leukemia-derived exosomes in plasma of patients
- Phenotype leukemia-derived exosomes
- Quantify exosomes from plasma of pediatric leukemia patents
- Screen for exosomal biomarkers originating from leukemic cells

3 MATERIALS AND METHODS

3.1 CLINICAL SAMPLES

Patients

Plasma was obtained from pediatric acute leukemia patients admitted at the Division of Children, Oslo University Hospital (OUH) after informed parental consent in the period 2016-2018. Blood samples (4 mL heparinized blood) were taken by study nurses according to the scheme depicted in figure 3.1. For ALL, samples were taken at diagnosis, twice during the initial intensive induction phase (day 15 and say 29), and after the induction phase and prior to the consolidation phase (day 79). We did not have samples at end of treatment, as none of the included patients had reached this point in their treatment plan when this study was done (the treatment for this group lasts 2.5 years). For AML, samples were taken at diagnosis, during the induction phase (on day 22 after 1 treatment course), and about mid-way through treatment ("under treatment", the exact time point varied due to personalized treatment regimens), and at end of treatment. The study has approval from the Regional Committee for Medical and Health Research Ethics (REK20131866) and includes children 0–18 years old.

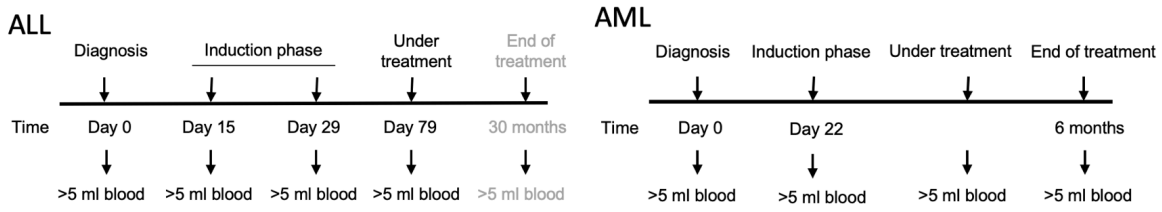

Figure 3.1: Overview of the sample collection timeline for pediatric leukemia patients, from day 0 (time of diagnosis), during the induction phase, during treatment (consolidation phase), and at end of treatment.

Healthy controls

Plasma from healthy pediatric controls were obtained from children undergoing elective surgery at Dep. of Pediatric Surgery, OUH after informed parental consent, and as part of routine blood sampling (REK20131866) (4 mL of heparinized blood).

Plasma from patients and healthy controls were separated and stored at -80°C prior to the start-up of this project (Lymphoprep separation of blood). An overview of patient and control

samples included in this thesis is provided in Appendix 2. The ALL group consists of one T-ALL and the rest are BCP-ALL.

3.2 EXOSOME ENRICHMENT USING SIZE-EXCLUSION CHROMATOGRAPHY.

This protocol was initially used to extract EVs from plasma samples. Plasma samples were separated through differential upstream centrifugation followed by 200 nm cut-off filtration to remove contaminants like larger vesicles and cell debris. To further reduce the sample complexity, the exosomes were enriched through size-exclusion chromatography on a sepharose CL-4B 10 mL mini-column obtaining fractions containing vesicles of exosomal size. Figure 3.2 presents a stepwise overview of the exosome enrichment protocol, from plasma to exosomal fractions.

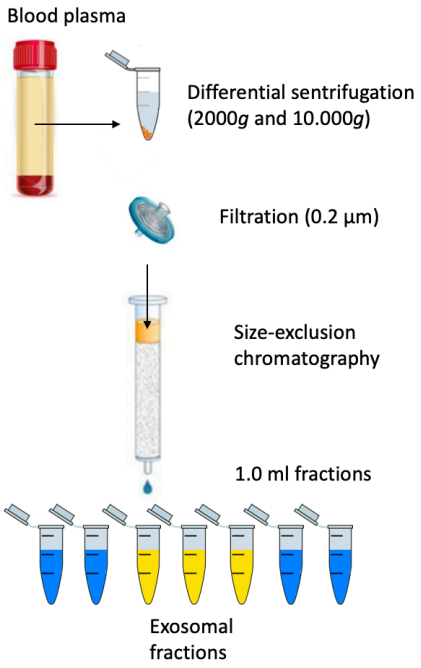

Figure 3.2 Overview of the main steps in the SEC-based exosomal enrichment protocol from plasma through differential centrifugation, filtration, and size-exclusion chromatography resulting in exosomes in fractions 3-5.

EQUIPMENT AND REAGENTS

Syringe, 10 mL (BD Biosciences, San Jose, CA)

3-way stopper, BD Connecta (BD Biosciences, San Jose, CA)

Sepharose CL-4B (Sigma-Aldrich, St Louis, MI)

Non-pyrogenic sterile-R filter, 0.22 µm (Sarstedt, Oslo, Norway)
dH_2O, filtered (0.22 µm cut-off)
PBS + 0.32 % trisodiumcitrate, filtered (0.22 µm cut-off) (Appendix 3)
20 % ethanol, filtered (0.22 µm cut-off)
Eppendorf tubes 1.5 mL (Sigma-Aldrich, St Louis, MI)

PROCEDURE

Preparation of mini-SEC column

The plunger was removed from the 10 mL syringe, and a filter inserted in the bottom of the syringe. A 3-way stopper was placed onto the syringe tip to control fluid flow. Sepharose CL-4B was then carefully poured into the syringe and let to settle at the 10 mL point where a second filter was added on top. One column volume (10 mL) of filtered dH_2O was added to the column to wash away excess ethanol from the sepharose. The SEC column was then equilibrated with 20 mL running buffer (PBS + 0.32 % trisodiumcitrate) before enrichment of small EVs. A small amount of running buffer was left over the filter to avoid drying of the column.

Preparation of plasma sample

Patient or healthy control plasma sample (~1.3 mL) was thawed, transferred to an Eppendorf tube and centrifuged at 2000*g* for 20 min at 4 °C. Without disturbing the pellet, the supernatant was transferred to a new Eppendorf tube, and centrifuged at 10.000*g* for 20 min at 4 °C. The supernatant was then filtered (0.22 µm) before it was transferred to a new Eppendorf tube and stored on ice until ready for use.

Enrichment of exosomes

Ten Eppendorf tubes were labeled with #1-10 and patient/control identifier (patients/controls numbered in the order samples were received, identification of person only possible by the study nurse/doctor). Remaining fluid was run through the SEC column. One mL of filtered plasma was added on top of the column and sunk into the sepharose before adding 12 mL PBS + 0.32% disodium citrate. At this point 10 fractions á 1 mL was collected. After each run, the column was washed using 20 mL filtered H_2O, followed by 10 mL filtered 10% ethanol. Some fluid was left above the filter, and the syringe was capped with parafilm before being stored in the fridge. Small EVs were found in fractions 3-5, with a peak in fraction 4. The eluates were stored at -20°C until use.

3.3 SAMPLE PREPARATION FOR IMAGESTREAM

3.3.1. LABELING SEC-FRACTIONS WITH FLUORESCENT DYE

While SEC enriches for exosomes, other contaminants of exosomal size, like protein aggregates and lipid complexes will co-elute in the fractions. To distinguish between bona fide exosomes and these contaminants, the SEC fractions putatively containing exosomes was stained with a fluorescent lipid-penetrable dye; carboxyfluorescein diacetate succinimidyl ester (CFDA-SE). Due to its acetate groups, CFDA-SE is highly permeable to lipid bilayers and will rapidly pass through cellular or vesicular membranes. Once the dye has crossed a membrane, esterases will cleave off the acetate groups converting it to carboxyfluorescein succinimidyl ester (CFSE) and thereby withholding it within the cell or vesicle. CFSE then serves as fluorescent molecule that will light up inside cells or vesicles, as illustrated in figure 3.3.

CFDA-SE was tested with filtered PBS alone to avoid false positive detection. Furthermore, Triton X-100 was used as a control to show loss of CFSE-signal when membranes of putative vesicles are destroyed. Triton X-100 is a commonly used detergent suitable for lysing of cells and will in this case permeabilize the exosomes making the fluorescent CFSE leak out.

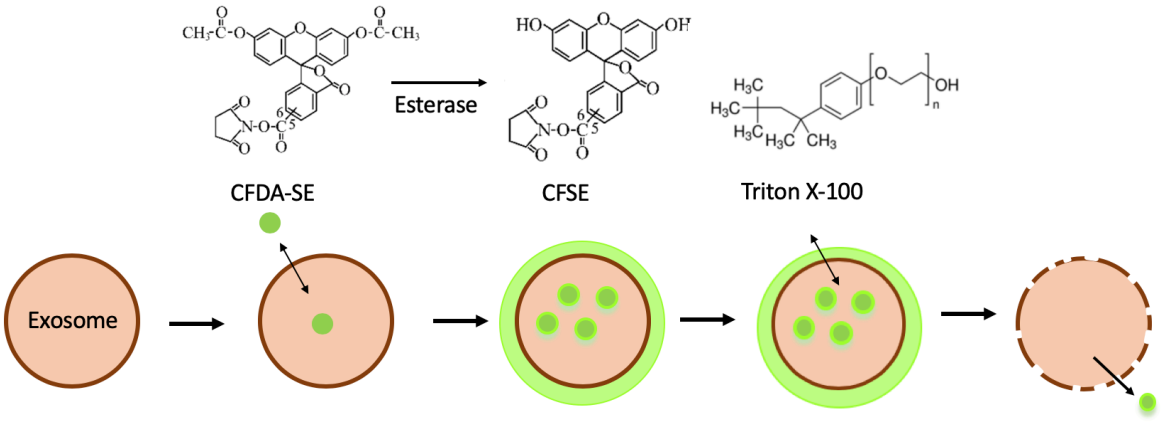

Figure 3.3 Schematic representation of the general process of fluorescent labeling of exosomes using CFDA-SE as well as the detergent Triton X-100.

3.3.2 STAINING WITH FLUORESCENT ANTIBODIES

By staining the samples with fluorochrome-conjugated antibodies it is possible to phenotype the exosomes. The purpose was to identify leukemia-derived exosomes. With this technique, only antigens located on the surface of the exosomes are available for antibody binding. To

avoid false positive events, all antibodies were run with filtered PBS alone to ensure antibody aggregates were not present.

3.3.3. IMAGESTREAM ANALYSIS

The image platform ImageStream^{x} (advanced imaging flow cytometer) was utilized to visually identify and quantify single exosomes by combing the fluorescent dye and antibodies with side and size scatter characteristics. The light scattering properties can distinguish exosomes from larger vesicles because of their small size not yielding any side scatter signal.

EQUIPMENT AND REAGENTS

Eppendorf 1.5 mL tubes (Sigma-Aldrich, St Louis, MI)
PBS buffer (filtered, 0.22 μm)
CFDA-SE cell tracer kit (Vybrant) (ThermoFisher, Waltham, MA)
10 % Triton X-100 (ThermoFisher, Waltham, MA)
Fluorescently labelled antibodies (see Appendix 4)
37 °C water bath
Amnis ImageStream^{X} (Luminex, Austin, TX)

PROCEDURE

90 μL of filtered PBS was transferred to an Eppendorf tube and 10 μL of exosome fraction (1 to 10) was added. Two samples were prepared for each fraction. CFDA-SE 10 mM stock solution was prepared as described in Appendix 3 and added to a final concentration of 10 μM. The samples were then incubated in a 37 °C water bath for 15 minutes. Afterwards, 12 μL of 10% Triton X-100 was added to one of the duplicates, while the other sample was stained with 2 μL of the desired antibodies. All samples were then incubated for 20 minutes, at room temperature, protected from light. The Triton X-100 sample was made to ensure that CFSE-detected signals were from vesicles. Negative controls with filtered PBS (90 μL) and exosome sample (10 μL) without addition of CFDA-SE was made, as well as only filtered PBS (90 μL) alone with antibodies (2 μL) to control for background noise from the antibodies.

ISx startup took about 45 minutes, which included instrument calibration which was performed automatically before each experiment. The ISx is equipped with 12 channels, channel 1 was automatically set to brightfield, channel 6 was set to side-scatter, and the rest are fluorescent

channels depending on the wavelength of our markers. The machine works best if the channels that are not required are turned off, this was done after selection of required channels. The machine extracted 15 µl of sample from the Eppendorf tubes, and up to 5000 events were acquired with fluidics set at low speed, sensitivity set to high, and magnification at 60x. Data analyses were performed using the ISx Data Exploration and Analysis Software (IDEAS).

3.4 EXOSOME ENRICHMENT USING EXOSOME PURIFICATION KIT

This technique was used to enrich for intact functional exosomes from blood plasma, using the Exo-spin™ technology. This procedure combines exosome precipitation with size-exclusion chromatography. Excess cells and cell debris were removed from plasma through a two-step centrifugation procedure prior to precipitation. The exosome-containing pellet was then resuspended and purified through a size-exclusion column. Figure 3.4 illustrates a stepwise overview of the purification protocol.

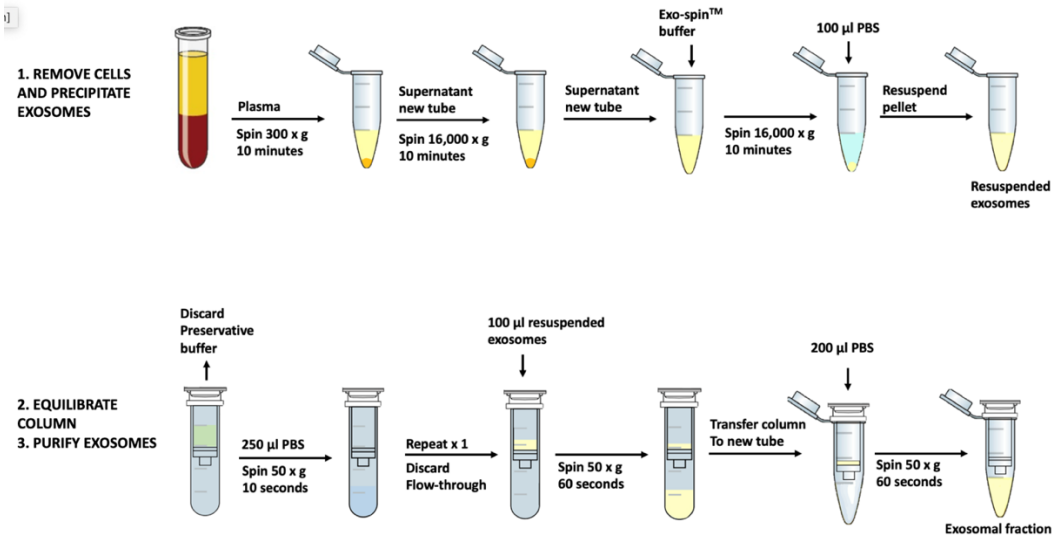

Figure 3.4: Flow chart illustrating the main steps of the Exo-spin exosomal purification protocol. Firstly, cell debris is removed through centrifugation before the exosomes are precipitated and resuspended in PBS. Secondly, the resuspended exosomes are purified through a size-exclusion column.

EQUIPMENT AND REAGENTS

Eppendorf tubes 1.5 mL (Sigma-Aldrich, St Louis, MI)

Exo-spin™ Buffer (Cell Guidance Systems, Cambridge, UK)

Exo-spin™ PBS (without calcium/magnesium, Cell Guidance Systems, Cambridge, UK)

Exo-spin™ spin-column (Cell Guidance Systems, Cambridge, UK)

Exo-spin™ waste collection tubes 2.0 mL (Cell Guidance Systems, Cambridge, UK)
Microcentrifuge (MicroStar 17R, VWR, Oslo, Norway)

PROCEDURE

The manufacturer's kit protocol was followed:

Removing cell debris

350 µl of blood plasma was transferred to an Eppendorf tube, and spun at 300*g* for 10 min at 4°C to remove cells. Supernatant was then transferred to a new Eppendorf tube, and spun at 16,000*g* for 30 min to remove any remaining cell debris and larger particles/vesicles.

Precipitation of exosomes

The supernatant (125 µl) was transferred to a new centrifuge tube, and Exo-spin™ Buffer was added in a 1:2 ratio (125 µl:250 µl), mixed by inverting and incubated at 4°C for 5 min, followed by centrifugation at 16,000*g* for 30 min at 4 °C. The supernatant was carefully aspirated and discarded, and the exosomal pellet was immediately (to avoid drying out of sample and damage of exosomes) resuspended in 100 µl of PBS (provided with the kit).

Preparation of Exo-spin™ SEC column

The SEC columns were equilibrated at room temperature for 15 min before use. The outlet plug was removed before the screw cap and the spin-column was placed into the collection tube provided. The preservative buffer from the top of the column was aspirated and discarded, and 250 µl of PBS was added immediately to prevent drying of the column bed. The column was then equilibrated by centrifugation at 50*g* for 10 sec, and this step was repeated once more (adding PBS and centrifuged) before proceeding. (If any PBS remained above the top filter, the spin was repeated for 5 seconds at the same speed.)

Purification of exosomes

100 µl of the resuspended exosomes were carefully applied to the top of the column, and the column was placed into the waste collection tube. The sample was centrifuged at 50*g* for 60 sec and the flow-through discarded. The column was then placed into a microcentrifuge tube and 200 µl of PBS was added to the top of the column. The tube with the column was then centrifuged at 50*g* for 60 sec to elute the purified exosomes. The tubes were stored at -20°C.

3.5 NANOPARTICLE TRACKING ANALYSIS

Nanoparticle tracking analysis (NTA) is a light-scattering method that allows particles within the size range of 10 - 1000 nm to be seen, measured, and counted. A laser beam is passed through a sample chamber and the illuminated particles will disperse light that is focused onto a 20x microscope with a video camera that records the Brownian motion of the particles (See figure 3.5 below). The NTA method is capable of measuring the size of each individual particle and can therefore count every particle that comes within the cameras field view. By using standard measurements, the camera field view is fixed and the laser beam depth set, making it possible to assess the concentration (scatter volume). The results are presented as particle size distribution plots as depicted in figure 3.5

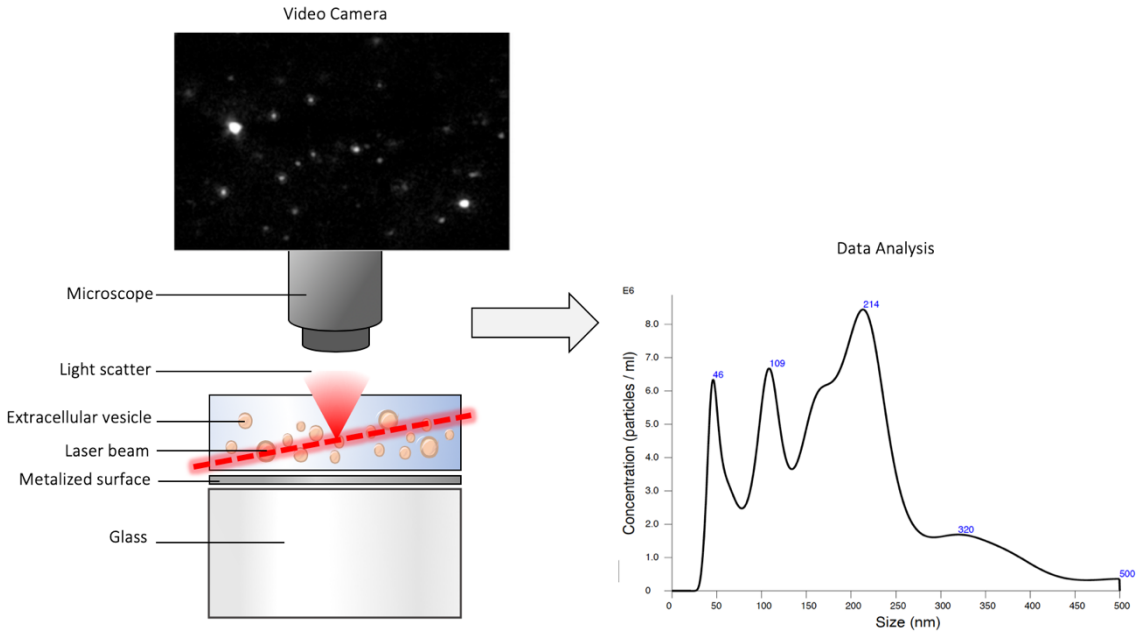

Figure 3.5: Illustration depicting the optical configuration and size distribution profile produced by NTA. The x axis shows the size in nm, and the y axis shows the count of individual particles per mL.

This single particle analysis technique was used to detect and enumerate EVs and validate exosomal content in our samples. Of the different NTA instruments produced by NanoSite, we have used the NS500 with automated sample introduction and handling.

EQUIPMENT AND REAGENTS

NanoSite NS500 (Malvern Panalytical, Malvern, UK)

dH_2O

PBS, filtered
Inorganic membrane filter, 0.02 μm
Polystyrene Size Standards, 100 nm
Syringe, 1 mL
Vortexer

PROCEDURE
Using NTA v3.4.54 software, the finite track length adjustment (FTLA) analysis script was set up with a 60 second measurement per sample and each sample was performed in triplicates.

To make sure the sample chamber was free from particles it was first cleaned by loading filtered PBS into the chamber with a 1 mL syringe. There should be no air bubbles in the syringe, as this can cause background scattering. The washing procedure was done between each sample injection. The machine was then calibrated using polystyrene beads (100nm) to control for instrument size measurement. All samples were diluted in filtered PBS to approx. 10^7-10^8 particles per mL and vortexed before they were transferred to the chamber by the 1 mL syringe. The camera level was set to 14 where the smallest particles were just visible, the infusion rate was set to 20, and the detection threshold to 3.

3.6 ELECTRON MICROSCOPY

To verify that we had exosomes in our fractions we sent one sample (BCP-ALL at diagnosis, P74) to the electron microscopy core facility at Oslo University Hospital for negative staining. Transmission electron microscopy (TEM) provides us with a magnified and focused image of our samples by a microscopy technique, which sends a beam of electrons through our samples and imaging at a high resolution. The exosomes are structurally verified by their cup-shaped morphology, which is a result of the dehydration and fixation during sample preparation.

3.7 EXOCET QUANTITATION ASSAY

The EXOCET quantitation kit was used to quantify exosomes after isolation by measuring the exosomal esterase activity through a colorimetric analysis. Colorimetric assays use spectrophotometry to measure the amount of light absorbed by a solution to predict the solutions concentration. This is based on Beer-Lamberts Law: The concentration of a solution is directly proportional to its absorption of light. Meaning a beam of light will become weaker as it passes

through a solution, and the higher the concentration, the higher the light absorbance will be. This is done by firstly measuring the absorbance of a series of known dilutions preferably from a solution similar to your own sample. A standard curve can then be made to find the unknown concentration of a sample by measuring its absorbance.

The EXOCET colorimetric assay is designed to measure the activity of esterases known to be highly enriched in exosomes, and the wavelength, which is specific to the reagent, reads at 450 nm. The EXOCET standard curve was calibrated to the signal from known exosome solutions (provided with the kit) and can be used to calculate the number of exosomes in a sample. The concentration can then be calculated by dividing the estimated number of exosomes (in the sample) by the volume of sample used.

EQUIPMENT AND REAGENTS

Eppendorf tubes (Sigma-Aldrich, St Louis, MI)
PBS (Appendix 3)
Exosome Lysis Buffer (provided with the kit, System Biosciences, Palo Alto, CA)
EXOCET Buffer A (provided with the kit, System Biosciences, Palo Alto, CA)
EXOCET Buffer B (provided with the kit, System Biosciences, Palo Alto, CA)
PBS-B Buffer (sterile, (provided with the kit, System Biosciences, Palo Alto, CA)
EXOCET standard (provided with the kit, System Biosciences, Palo Alto, CA)
96 well assay plate (12x8 strips) (provided with the kit, System Biosciences, Palo Alto, CA)
Microcentrifuge (MicroStar 17R, VWR, Oslo, Norway)
Spectrophotometer (Multiskan Ascent plate reader, ThermoFisher, Waltham, MA)

PROCEDURE

The manufacturer's protocol was followed. Buffers were brought to room temperature before use.

Exosomal sample preparation

30 µL of the exosome sample (approximately 20 - 100 µg exosomal protein per reaction) was mixed with 70 µL of lysis buffer in Eppendorf tubes before incubation at room temperature for 5 minutes to liberate the exosomal proteins. The samples were vortexed for 15 seconds followed

by a 5-minute centrifugation at 15,000*g* to remove debris. The supernatant was then transferred to a new tube on ice.

Standard curve preparation

We made a serial dilution (1:2) of the EXOCET standard with PBS-B buffer in centrifuge tubes.

Reaction buffer preparation

Reaction buffer was prepared by mixing 50 µL of buffer A with 0.5 µL of buffer B for each reaction.

EXOCET assay

In each well of a 96-well plate, we added 50 µL of reaction buffer and 50 µL of standard or exosome sample. The plate was incubated for 10-20 minutes at room temperature, and immediately analyzed using a spectrophotometric plate reader at 450 nm.

3.8 BCA PROTEIN ASSAY

The Pierce™ BCA Protein Assay Kit was used to quantify the amount of protein in our samples through colorimetric detection. This should give an overview of how much protein the isolated exosome samples contain, implying that a higher protein concentration indicates a higher number of exosomes. This colorimetric technique is detergent-compatible and primarily based on two reactions. Firstly Cu^{2+} is reduced to Cu^{+} by the peptide bonds in an alkaline solution. Secondly a violet-colored complex is formed by the chelation of two bicinchoninic acid (BCA) molecules with each cuprous ion (Cu^{+}). The violet product exhibits a strong absorbance at 562 nm that is almost linear for increasing protein concentrations between a working range of 0.02-2 mg/mL. Quantitation of protein present in a sample is then done by measuring the absorption spectra and comparing it with a reference protein of known concentrations.

EQUIPMENT AND REAGENTS

Spectrophotometer (Multiskan Ascent plate reader, ThermoFisher Scientific, Waltham, MA)
Flat bottom, 96 well microtiter plate (ThermoFisher Scientific, Waltham, MA)
Eppendorf tubes (Sigma-Aldrich, St Louis, MI)
PBS (Appendix 3)
Triton X-100 (10%) (ThermoFisher Scientific, Waltham, MA)

Albumin standard ampules, 2 mg/mL (ThermoFisher Scientific, Waltham, MA)
BCA reagent A (ThermoFisher Scientific, Waltham, MA)
BCA reagent B (ThermoFisher Scientific, Waltham, MA)

PROCEDURE
We followed the manufacturer's protocol:

BSA standard preparation
Firstly, a serial dilution (1:1) of the BSA with PBS buffer was made. We started by marking 7 centrifuge tubes with the letters A to G and then added 200 µL BSA 2mg/mL to tube A. We then added 100 µL PBS to tubes B through to G and started transferring 100 µL from A to B, mixing, and continuing from B to C and so on.

Exosomal sample preparation
The lysis buffer was made by mixing 2.5 µL of 10 % Triton X-100 with 20 µL of PBS per reaction. Then 22.5 µL of lysis buffer was added to 2.5 µL of exosome sample and incubated for minimum 10 minutes at room temperature.

Working reagent preparation
Created a sufficient amount for the assay, mixed and used it within one hour. Combined 200 µL of buffer A (bicinchoninic acid) with 1/50 volume of buffer B (cupric sulfate) for each reaction.

BCA protein assay
In each well of a 96-well plate, 25 µL of standard or exosome sample was added, and then 25 µL of working reagent was added to all samples. The plate was incubated for 20 minutes at 37 °C and analyzed at 570 nm using a spectrophotometer.

3.9 SDS-PAGE AND WESTERN BLOTTING

This protocol was used to identify exosomal proteins after isolation. Western blot is a qualitative and semi-quantitative technique, able to identify the presence of specific proteins in a sample.

SDS-PAGE separates proteins on the basis of their molecular weights. To release the proteins from the membrane enclosed exosomes lysis is performed at a low temperature to avoid denaturation of proteins, and a protease inhibitor is added to prevent protein degradation. To make the proteins denature and impart a net negative charge the anionic detergent SDS is added. To further linearize the proteins into polypeptides, the disulfide bridges that make up the proteins secondary structure are broken by adding a reducing agent. Now that all proteins are linear and negatively charged, the difference in electrophoretic mobility will be based solely on their molecular weights. Shorter proteins will move faster through the pores of the gel and larger proteins will move slower due to greater hindrance. The acrylamide concentration can vary, generally in a range between 5 - 25 %, and determines the resolution of the proteins. High concentration gels are used to resolve low molecular weight proteins, while low percentage is better for larger proteins.

Western Blotting transfers the separated proteins present on the gel onto a membrane. This is achieved through a gel-membrane sandwich were an electric current is applied and the negatively charged proteins will migrate towards the membrane as they move to the positive terminal. Through hydrophobic interaction, the proteins then bind to the membrane, maintaining their original position and concentration. The proteins of interest are exposed through a process called indirect detection, where two types of antibodies are utilized. Firstly, primary antibodies are added to mark the target proteins and secondly, a secondary antibody, tagged with a reactive enzyme (horse radish peroxidase, HRP) is used to bind the first antibody. The specific antigen-protein complex can then be measured by adding a substrate solution (ECL) containing luminol and peroxide. In this case, the HRP enzyme (on the 2nd antibody) will oxidize luminol in the presence of peroxide, resulting in the luminol emitting light and enabling visualization of the complex by autoradiography.

EQUIPMENT AND REAGENTS

Triton X-100, 10 % (ThermoFisher Scientific, Waltham, MA)
Protease inhibitor cocktail (Roche, Basel, Switzerland)
Lysis buffer (300 mM NaCl/ 50 mM Tris, pH 7.4, Appendix 3)
Eppendorf tubes 1.5 mL (Sigma-Aldrich, St Louis, MI)
Heat block at 95 °C
12 % Tris-Glycine 18-well gels (Criterion^{TM} TGX precast Gels) (Bio-Rad, Uppsala, Sweden)

1 x SDS running buffer (Appendix 3)

Precision Plus protein™ Dual color standards (Bio-Rad, Uppsala, Sweden)

4 x SDS loading buffer (Appendix 3)

Semi-dry transfer apparatus, TE 70 ECL Semi-dry Transfer Unit (Amersham Biosciences)

Western blotting filter paper, extra thick Filter (Bio-Rad, Uppsala, Sweden)

PVDF membrane (Merck Millipore, Burlington, MA)

Methanol (Sigma-Aldrich, St Louis, MI)

Transfer buffer (Appendix 3)

dH_2O

TBS-Tween (Appendix 3)

Blocking buffer (Appendix 3)

Antibodies of interest (see Appendix 4)

HRP-conjugated secondary antibodies (See Appendix 4)

SuperSignal® West Pico Luminol/Enhancer solution (ThermoFisher Scientific, Waltham, MA)

SuperSignal® West Pico Peroxide solution (ThermoFisher Scientific, Waltham, MA)

ChemiDoc™MP Imaging system (Bio-Rad, Uppsala, Sweden)

Image Lab 4.1 (BioRad, Uppsala, Sweden)

PROCEDURE

SDS-PAGE

2x lysis buffer was made by mixing 200 µL of 10 % Tx-100 with 750 µL NaCl/Tris-HCl and 20 µL protease inhibitor cocktail. 10 µL of lysis buffer was added to 10 µL exosome sample, mixed, and incubated on ice for 10 minutes before centrifugation at 17,000*g* (4 °C) for another 10 minutes. The supernatant was added to a new centrifuge tube and mixed with 10 µL of loading buffer (4 x SDS loading buffer) before boiling on heat block (95 °C) for 2 minutes. The sample was cooled on ice before gel electrophoresis.

The wells of the gel were rinsed in milliQ water before the gel was placed into the electrophoresis chamber, and the chambers (upper and lower) filled with SDS running buffer. The molecular weight marker (2 µl) and exosomal samples (20 µl) were then loaded into appropriate wells, and the gel run at 200 V for 50 minutes.

WESTERN BLOT

The PVDF membrane was cut to size, and activated by a 20 second soak in methanol, followed by a milliQ water rinse (1 minute), and placed in transfer buffer. Two thick blotting filter papers, and the finished SDS gel, were also soaked in transfer buffer. The following sandwich was composed in the semi-dry transfer apparatus from bottom to top: filter - PVDF membrane - gel – filter, and run at 100 mA for 1 h and 5 min. After transfer, the membrane was soaked in TBS-Tween making sure the side that was in contact with the gel was facing up. The TBS-Tween was replaced with blocking buffer and the membrane incubated for 1 h on a rocker at room temperature. The blocking buffer was then removed and replaced with a primary antibody (see Appendix 4) in 5 % skimmed milk and incubated for 1 hour on a rocker at room temperature (or overnight at 4°C). The primary antibody was then removed by washing the membrane 3 x 5 minutes in TBS-Tween. The secondary antibody (see Appendix 4) was diluted in TBS-Tween and added to the membrane and incubated for 1 hour at room temperature while shaking. This was followed by another membrane wash for 3 x 5 minutes. The membrane was developed using the ECL substrate. 2 mL of luminol was mixed with 2 mL of peroxide and added on the membrane for 1 minute to activate the HRP-enzyme. The resulting signals was detected using a ChemiDoc^{TM}MP Imaging system using different exposure times.

3.10 ANTIBODY ARRAY ANALYSIS

An antibody array assay was used to screen for proteins in the exosomal samples. This method combines protein detection using antibody arrays and protein size separation by SDS-PAGE. The antibody array analysis is based on detection of soluble biotinylated proteins using antibodies coupled to bar-coded fluorescently labeled beads. The antibody/bead-captured biotinylated proteins are detected with fluorescently labeled streptavidin. Fluorescence intensity of the streptavidin signal would then measure the level of target proteins in the sample. With this method, proteins are first biotinylated before they are separated by size through SDS-PAGE and transferred onto nitrocellulose membrane. The membrane is then cut into 48 vertical strips, representing different protein sizes, and the proteins are then eluted off from the membrane pieces. The protein solutions are then mixed with antibody arrays consisting of individual color-coded beads and then analyzed using a flow cytometer. The typical dot plot of the flow cytometry data shows the bar-coded beads and the intensity of any captured protein as a fluorescent streptavidin signal. Figure 3.6 provides an overview of the antibody bead array method.

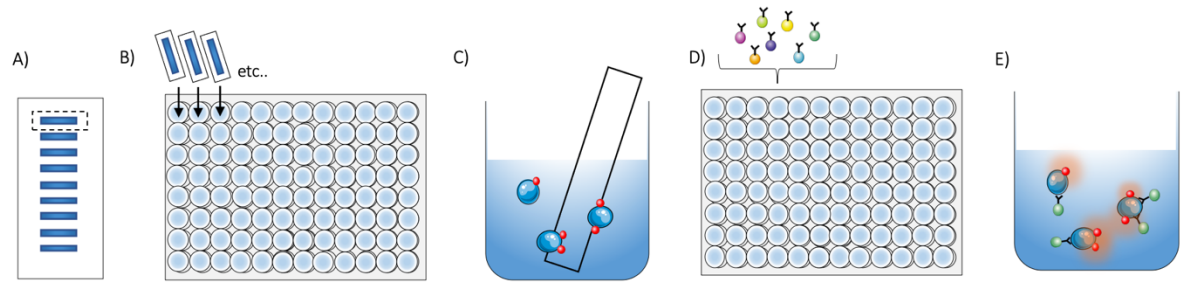

Figure 3.6: Overview of the main steps of the antibody array assay protocol. A) Exosomal biotinylated proteins are separated by SDS-PAGE and transferred to a membrane. B) Each lane/sample is cut into 48 pieces and transferred to a 96-well plat, one piece per well, total 48 wells per sample. C) The biotinylated proteins (biotin indicated in red dots) are then eluted from the membrane, giving 48 wells with soluble proteins separated according to size. D) Antibody arrays are added to each well, and the antibodies bind to their target proteins if these are present. E) Unbound proteins are washed away, and captured proteins can be detected via biotin-streptavidin-PE.

EQUIPMENT AND REAGENTS

Sample preparation and biotinylation

Triton X-100, 10 % (ThermoFisher, Waltham, MA)

Protease inhibitor cocktail (Roche, Basel, Switzerland)

300 mM NaCl/ 50 mM Tris, pH 7.4 (Appendix 3)

Eppendorf tubes 1.5 mL (Sigma-Aldrich, St Louis, MI)

Heat block 95 °C

Biotin, 100 µg/mL (Sigma-Aldrich, St Louis, MI)

SDS-PAGE

4 - 20 % Tris-Glycine gel, 12-well (Criterion™ TGX precast Gels) (Bio-Rad, Uppsala, Sweden)

1 x SDS running buffer (Appendix 3)

Precision Plus protein™ Dual color standards (Bio-Rad, Uppsala, Sweden)

4 x SDS loading buffer (Appendix 3)

Transfer

PierceG2 Fast blotter (Thermo Scientific, Waltham, MA)

Thin blotting filter paper (Bio-Rad, Uppsala, Sweden)

Nitrocellulose membrane, 0.45 µm (Bio-Rad, Uppsala, Sweden)

Pierce 1-step Transfer buffer (ThermoFisher Scientific, Waltham, MA)

0.1 % Ponceau S in 1% acidic acid (Sigma-Aldrich, St Louis, MI)

dH_2O

Cutting of membrane and protein elution

Shape cutter (Fiskars, Finland)

Tweezers

PBS-Tween (Appendix 3)

Urea elution buffer (Appendix 3)

dH_2O

PCR plate (Sigma-Aldrich, St Louis, MI)

96 well V-bottom plate (ThermoFisher Scientific, Waltham, MA)

Eppendorf MixMate (Eppendorf, Hamburg, Germany)

Antibody array preparation

Bead-block buffer (Appendix 3)

Antibody array (100 µL) (made by the Lund-Johansen lab, Oslo University Hospital)

1.5 mL Eppendorf tube

Flow cytometry analysis

PBS + Tween with 5 % BSA

BD Fortessa flow cytometer (BD Biosciences)

PROCEDURE

Sample preparation by lysis

Lysis buffer (2.5 µL) was added to 25 µL of exosome sample, the sample was mixed, and incubated at 95°C for 3 min, and thereafter placed on ice. Samples were centrifuged at 17,000*g* (4°C) for 5 min and the supernatant transferred to a new Eppendorf tube. Samples were biotinylated by adding 1 µL of a 100 µg/mL of biotin stock solution to each sample and incubated for 1 hour on ice.

SDS-PAGE

Each sample was mixed with 6 µL loading buffer (4 x SDS loading buffer) before they were loaded (20 µL) into appropriate wells, and the gel run at 100 V for 90 minutes.

Transfer

The nitrocellulose membrane and the filter papers were briefly soaked in transfer buffer before stacking from bottom to top: filter - membrane - gel – filter and run for 12 min in a fast blotter apparatus. After transfer the membrane was stained with 0.1 % Ponceaus S in 1% acidic acid for 5 minutes to visualize the protein bands. Surplus color was washed away with dH_2O, and the membrane was left to dry overnight between two filter papers under pressure.

Cutting of bands

Each sample lane on the membrane was cut into 48 strips using a paper cutter coupled to a computer software. Each strip was added to a separate well of a 96-well PCR plate using a tweezer. The membrane strips were then de-stained through a 10 min incubation in 1 % PBS with 0.1 % Tween-20, and thereafter washed 3 times in dH_2O. Solutions were exchanged by manual pipetting.

Antibody Array preparations

A vial of frozen pre-made antibody bead-array (100 µL) was thawed and transferred to a 1.5 mL Eppendorf tube and added 1 mL PBS + 0.1 % Tween-20. The beads were spun down at maximum velocity for 1 min. The supernatant was removed, and the beads resuspended in 1 mL bead block buffer (to block unspecific binding).

Plate preparations

Urea elution buffer (15 µL) was added to each well, and the plate was incubated on a shaker for 90 minutes at 1700 rpm at room temperature to elute the proteins from the membrane. Then 200 µL of filtered (0.22µm) PBS-Tween containing 5 % BSA was added to each well, and the samples were transferred to 96-well V-bottom plate. Lastly, 10 µL of the antibody array was added to each well. The plate was incubated overnight, rotating, in a cold room.

Streptavidin binding

Unbound proteins were removed by centrifugation for 1 min at 1400 rpm, and the supernatant discarded. The beads were washed by adding 200 µL of PBS-Tween and centrifugation for 1 min at 1400 rpm, and the supernatant discarded. This was repeated 2 times. Captured biotinylated proteins were then stained with 20 µL of streptavidin-PE and incubated on a shaker

for 20 min at room temperature. Unbound streptavidin was then removed by washing, by adding 180 µL PBS-Tween and centrifugation for 1 minute at 1400 rpm, and the supernatant discarded. In the last step, 100 µL PBS-Tween + 5 % BSA, and the samples were run on a flow cytometer.

Sample analysis by flow cytometry

10.000 events from each well was acquired by the flow cytometer, using software with pre-set gates for the array. The data files were exported as .fsc files and analyzed using a pipeline of R tools and Excel commands in the Lund-Johansen lab.

3.11 STATISTICAL ANALYSIS

Data are expressed as mean ± standard deviation, using GraphPad Prism (GraphPad Software, USA). The statistical analyses were performed by unpaired non-parametrical t-tests as indicated. P-values of 0.05 or less were considered to be statistically significant.

4 RESULTS

4.1 CHARACTERIZATION OF SMALL EVS IN PLASMA OF ACUTE LEUKEMIA PATIENTS

4.1.1 SMALL EV DETECTION USING IMAGESTREAM TECHNOLOGY

Small EVs were extracted from plasma through up-stream differential centrifugation followed by a 200 nm cut-off filtration and size-exclusion chromatography. The fractions containing most small EVs were previously shown to be in fractions 3, 4, and 5 (35). To visually identify the small EV-content of the SEC-fractions, we utilized the image platform ImageStream^X. As previously discussed, the ImageStream^X instrument can detect particles down to 50-100 nm in size, by combining the technologies of fluorescence microscopy and flow cytometry.

To distinguish between EVs and contaminants like lipid complexes and protein aggregates, the fractions were stained with the fluorescent lipid-penetrable dye CFDA-SE. The dye permeates the vesicular lipid bilayer, gets cleaved by internal esterases, and converted to CFSE which ends up being withheld inside the vesicles and lighting them up. Due to their small size, small EVs will not yield any side scatter and anything above zero in scatter signal is interpreted as contaminants and debris. By gating on negative side scatter, and CFSE positive events, we could further characterize the exosomal vesicles. As exosomes are known to be enriched for the tetraspanin CD63, the samples were stained with PE-conjugated anti-CD63 antibodies.

Figure 4.1A shows the strategy for detecting exosomes by ImageStream. No CFSE-signal was detected in filtered PBS alone (the buffer used to prepare samples for ImageStream), while a potent CFSE-signal was shown in a sample containing Fraction 4. Disruption of the lipid bilayer using the detergent Tx100 resulted in loss of CFSE-signal in Fraction 4, indicating that the CFSE-signal indeed comes from vesicular structures. No background fluorescent activity was detected in the Fraction 4 sample without CFDA-SE added. To detect CD63, a PE-conjugated anti-CD63 antibody was used together with CFDA-SE. As seen in Figure 4.1B, we could detect particles that stained positive for both CFSE (green) and CD63 (yellow). Finally, in Figure 4.1C, we show data from one healthy control and one BCP-ALL patient, where it may seem that healthy controls have less $CFSE^+$ $CD63^+$ exosomes than the patient. However, more data is needed to confirm this. It is also clear from the data that only a minority of the $CFSE^+$ events

stained positive for CD63. Unfortunately, the ImageStream machine broke down at this point in the study (with 4 months left), and we had to abandon further planned experiments.

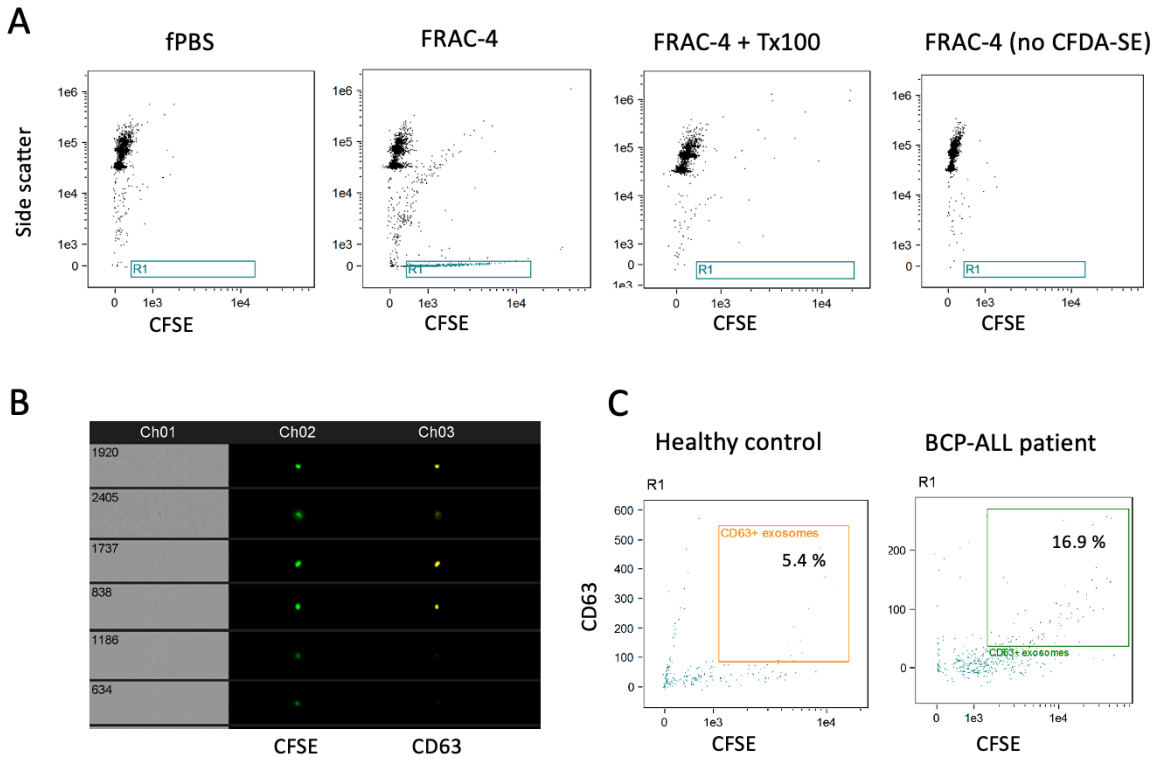

Figure 4.1: Detection of exosomal content using the imaging platform ImageStream^{x}. A) Gating strategy with CFSE positive events on the x-axis and side scatter on the y-axis using fPBS only in the first panel and then SEC fraction 4 from a healthy control. B) Identification of double positive vesicles using antibody labeling CD63 (in yellow) together with CFDA-SE (in green) on SEC fraction 4 from a healthy control. C) Gated exosomes (R1 gate) combining CFDA-SE and CD63 in one healthy control vs one BCP-ALL patient as indicated. fPBS: filtered PBS.

4.1.2 Small EV detection using conventional methodology

As the ImageStream approach had to be abandoned as a tool to quantify and phenotype small EVs, we chose to quantify small EVs using three more conventional methodological approaches; 1) BCA assay (total protein content measurement), 2) EXOCET assay (colorimetric method based on detection of an exosomal enzyme), and 3) NTA (particle counts). Further, we streamlined the isolation of small EVs by using the kit Exo-spin^{TM}, which combines precipitation with SEC. With this approach, we could isolate small EVs from 48 samples under the same conditions. We isolated small EVs from 10 healthy controls, and from 4 AML patients and 8 ALL patients at diagnosis and at different time points during treatment. See Appendix 2 for details.

NTA was performed to measure the size distribution profile of the samples. Each individual particle within the size range of 10 - 1000 nm is detected and counted with this method. Figure 4.2A shows the size distribution of particles in healthy controls (n=6), AML (n=4), and ALL (n=8) at diagnosis. The machine was only available a limited amount of time (1 day), which is why we did not get to run all the 48 samples. The data confirms that there are particles of EV size in our samples, but we detected very few particles in the size range of exosomes (50-100 nm). The figure is based on the average mode size of each sample and indicates that the vesicles isolated from controls and patients have approximately the same particle size distribution of about 100 - 150 nm. The mean value for each of the groups does seem to vary, with the controls having a slightly lower mean of about 130 nm and the patients being closer to 150 nm, however this difference is not significant. Figure 4.2B-C shows examples of the size distribution profile from one representative individual for each sample group; one healthy control, one AML and one ALL patient at diagnosis. The graphs show the samples containing particles of the same size range, but in different concentrations.

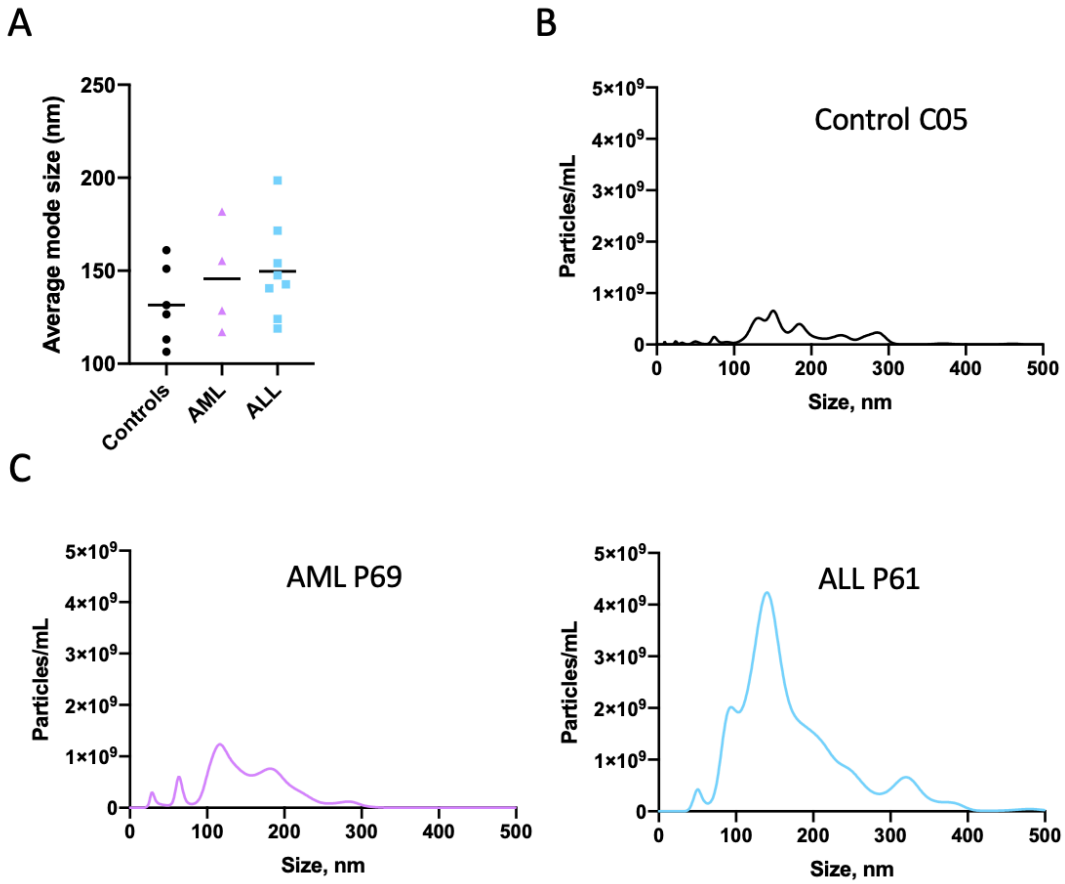

Figure 4.2 NTA size distribution profile of the samples. Panel A) Size analysis showing the average size in nm (mode) in healthy controls (n=6), and in AML (n=4) and ALL (n=8) patients at diagnosis. No statistical significance was detected between the groups. Panel B) Size distribution plot from one representative healthy control. Panel C) Size distribution plot from one representative AML patient and ALL patient at diagnosis.

To confirm that our samples contained exosomes we did transmission electron microscopy (TEM). Figure 4.3 shows two representative EM images from a total of eight images. The image to the left depicts predominantly small lipoproteins (white arrows). The image to the right verified successful isolation of exosomes (depicted by black arrows) by their characteristic cup-shaped morphology. Indicated by the size bars (black and white 100 nm each), the vesicles are about 80-150 nm in size and some of them seem to have aggregated (thick black arrow).

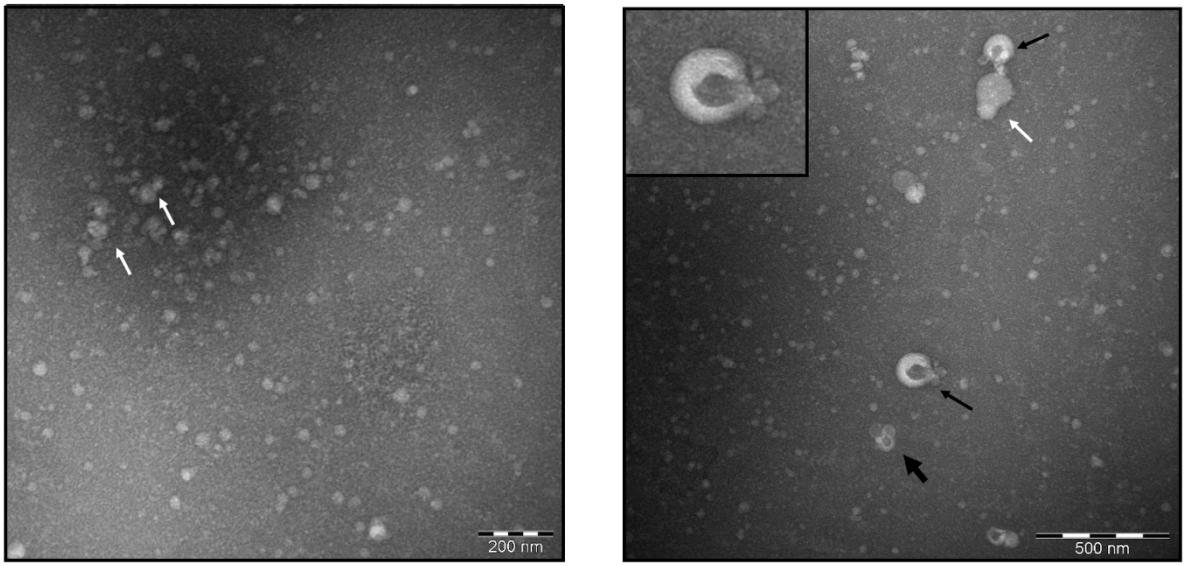

Figure 4.3: Negative stain transmission electron microscopy (TEM) from one exosomal fraction. Both images are from the same sample, where the image to the left illustrates plasma lipoproteins indicated by white arrows, and the right image shows particles with the characteristic cup-shaped features of exosomes indicated by black arrows. Enlarged small EV shown in top left of the last image. Size bars: 200 nm and 500 nm.

Having verified particles of small EV size and found cup-shaped exosomal vesicles in our samples, we continued further analysis to test for exosomal origins of these vesicles. As exosomes are known to be enriched in tetraspanins CD63 and CD81, a western blot analysis was set up to test for these markers. Here the EV-isolates were lysed to release the membrane bound and intravesicular proteins, the proteins separated by size using SDS-PAGE, and then transferred onto a membrane to be probed with the specific antibodies.

Figure 4.4 support the presence of exosomes by showing weak bands for CD63 and CD81 in both BCP-ALL patients and control samples. For the AML, on the other hand, these proteins seem to be expressed only in half of the patients. The BCP-ALL data shows an interesting finding where it seems to be a trend towards higher amounts of CD81 at diagnosis, which then decreases during treatment and is replaced by a higher expression of CD63 at day 79. The

signals are overall weak, which could reflect a heterogenous mixture of different populations of small EVs and lipoproteins in addition to exosomes. Also, we tested very small amounts of samples by Western blot, due to limited material available.

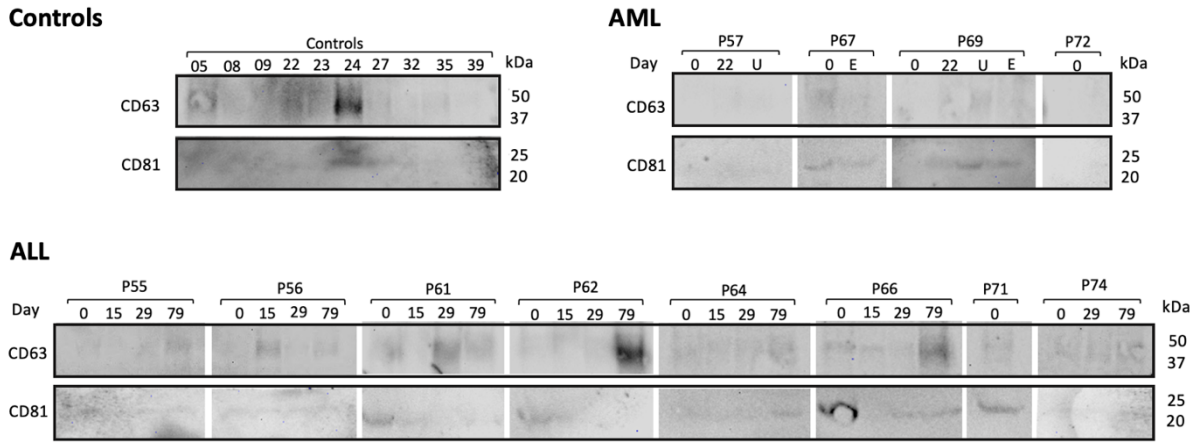

Figure 4.4 Western blot showing expression of CD63 and CD81 in samples isolated from plasma from healthy controls, BCP-ALL patients (except P71 that is T-ALL) and AML patients. ALL samples are from day 0 (at diagnosis), day 15 and 29 during induction phase and day 79 after induction phase. AML samples are from day 0 (at diagnosis), day 22, under treatment (U, after 2-3 rounds of induction), and end of treatment (E). Equal amount of exosome isolate was loaded (10 µl).

Finally, we investigated whether we could detect expression of the B-cell marker CD19 as well as the hematopoietic stem cell marker CD34. Both markers should be present on BCP-ALL cells. Figure 4.5A shows CD19 being expressed in all the samples, both from patients and controls. Expression levels on western blot was quantified by ImageJ, and the obtained signal values were normalized against the measured protein concentrations from the BCA assay (Fig. 4.5A, lower panel). This was done to control for varying amounts of EVs/proteins in the samples, since equal volumes of exosome isolates was loaded. The relative signals of CD19 was surprisingly lower in the ALL patients compared to controls ($p = 0.02$), and no statistical difference ($p = 0.1$) was observed between the controls and AML patients (Fig. 4.5B). For CD34, we observed (Figure 4.5C) a tendency towards higher expression in the patient groups, with a statistical significance ($p = 0.006$) between ALL and the controls, but no statistical difference ($p = 0.06$) between AML and the controls (Fig. 4.5D).

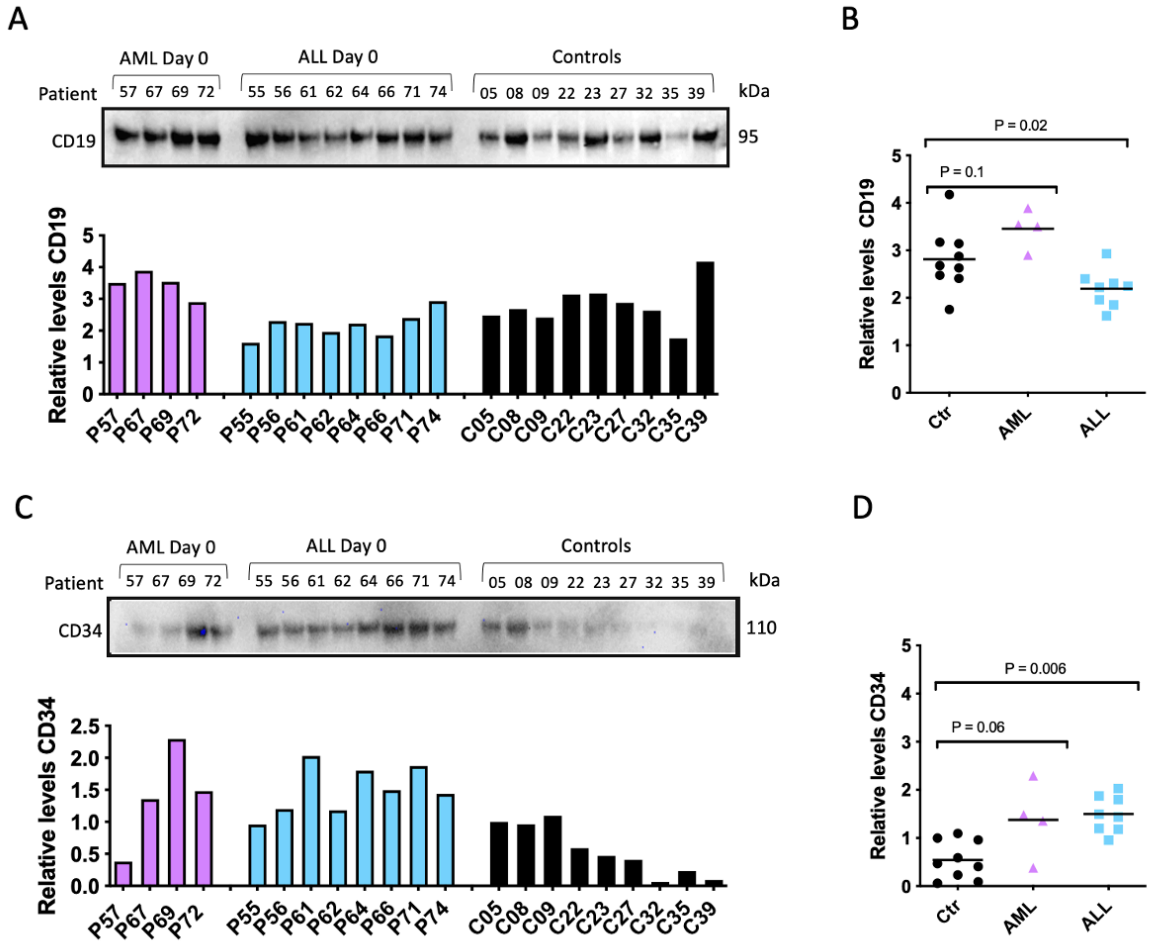

Figure 4.5 Western blot analysis of the B-cell marker CD19 and stem cell marker CD34. A) CD19 expression by Western blotting and corresponding relative expression levels normalized against protein concentration (BCA). B) Relative expression of CD19 in controls, AML, and ALL patients. C) CD34 expression by Western blotting and corresponding relative expression levels normalized against protein concentration (BCA). D) Relative expression of CD34 in controls, AML, and ALL patients. Statistical difference is quantified by an unpaired non-parametrical t-test, and p-values are indicated in the graphs. Equal amount of sample was loaded (10 µl). Black dots: controls. Purple dots: AML patients. Blue dots: ALL patients.

4.2 QUANTIFYING EXOSOMES IN PATIENTS AT DIAGNOSIS AND DURING TREATMENT

Having verified small EVs in our samples we continued further analysis to test if the patients have an increased exosomal load compared to healthy controls by using three different quantifying methods: BCA, EXOCET, and NTA. The BCA protein assay was used to quantify the amount of total protein in the exosomal samples, implying that a higher protein concentration potentially indicates a higher number of exosomes. The EXOCET quantitation kit is a colorimetric assay designed to measure the activity of esterases known to be enriched

in exosomes. And finally, the NTA analysis measures individual particles within the camera's field view, making it possible to assess the concentration in particles/mL.

The BCA assay (Figure 4.6 A) indicates an equivalent protein content in the samples from AML and the healthy controls as there is no statistically significant difference between the two. The ALL samples on the other hand shows increased protein concentration compared to the controls ($p=0.0155$). A higher protein concentration could indicate a higher number of small EVs. Figure 4.6B presents the EXOCET assay indicating a comparable exosome content between the patients, both AML and ALL, and the controls with no significant difference in the number of exosomes per µL plasma. For the NTA assay (Figure 4.6C), we found a higher particle content per mL in the patient samples contra the healthy controls. Both AML and ALL-groups are statistically significantly different ($p<0.05$) from the control group, and thus resembles the BCA results in Figure 4.6A. This suggest a pattern of higher EV content in the patients and can likely be generalized to a larger population study.

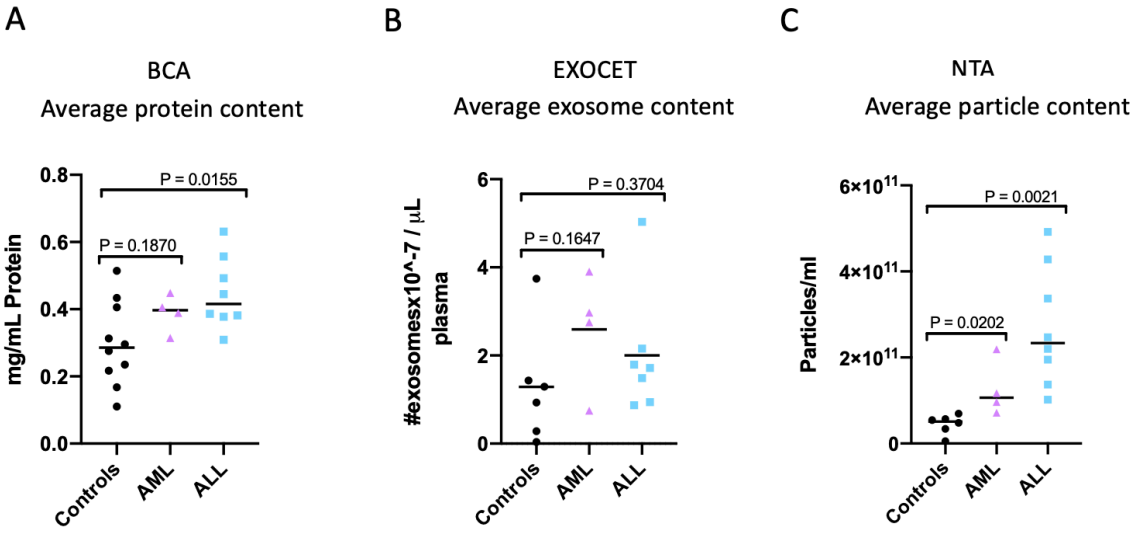

Figure 4.6 Quantification of EV content in healthy controls and patients at diagnosis using three different methods. A) BCA assay, healthy controls (n=10), AML (n=4), BCP-ALL (n=8). B) EXOCET assay, healthy controls (n=6), AML (n=4), BCP-ALL (n=7). C) NTA assay, healthy controls (n=6), AML (n=4), BCP-ALL (n=8). Horizontal bars indicate the mean of each group. Statistical significance was calculated using the non-parametrical Mann-Whitney t-test using GraphPad software.

As the outcome of the 3 different quantification tests showed varied results, we compared the three methods against each other. Based on data from Figure 4.6, we anticipated a correlation

between the BCA and the NTA assay. However, as shown in Figure 4.7B, we only found a weak correlation between these two assays ($r = 0.33$, p = 0.18). Surprisingly, the EXOCET and BCA data (Figure 4.7A) showed better correlation ($r = 0.43$, p = 0.08), and as expected there was no correlation observed between the EXOCET and NTA analysis (Figure 4.7C).

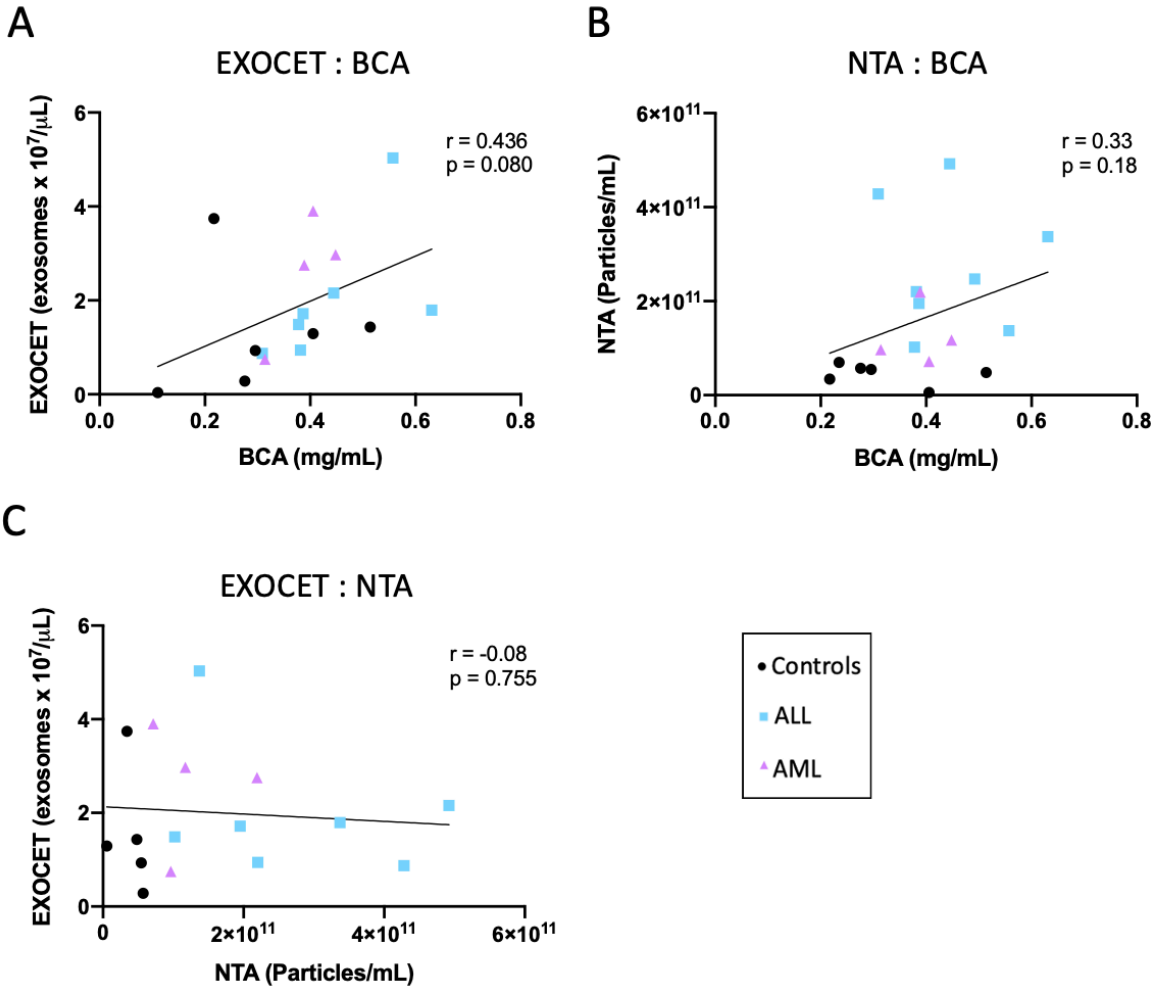

Figure 4.7: Correlation plots between the three different quantifying methods. A) Comparison of EXOCET vs BCA showing correlation between the two ($r = 0{,}43$, p = 0.08) B) Comparison of NTA vs BCA with a weak correlation ($r = 0.33$, p = 0.18) C) Comparison of EXOCET vs NTA with no correlation. Correlation was calculated using non-parametrical Spearman's correlation. Black dots: controls. Purple dots: AML patients. Blue dots: ALL patients.

We next investigated whether the sEV content would change during the course of treatment, hypothesizing that the number of sEVs in general would fall. We had a limited number of samples from AML patients taken during treatment, so this analysis was only done for the ALL patients. In Figure 4.8A-C it is demonstrated that there is no apparent difference in the amount of sEV content as measured by either BCA, EXOCET, or NTA. Due to differences in

measurements between individuals, we also calculated the relative change between the day of diagnosis (set as initial value) and set days during the treatment course (Figure 4.8D-F). We found no statistically significant difference between any of the treatment days compared to time of diagnosis with any of the tests. However, again, the number of patients for this analysis is low.

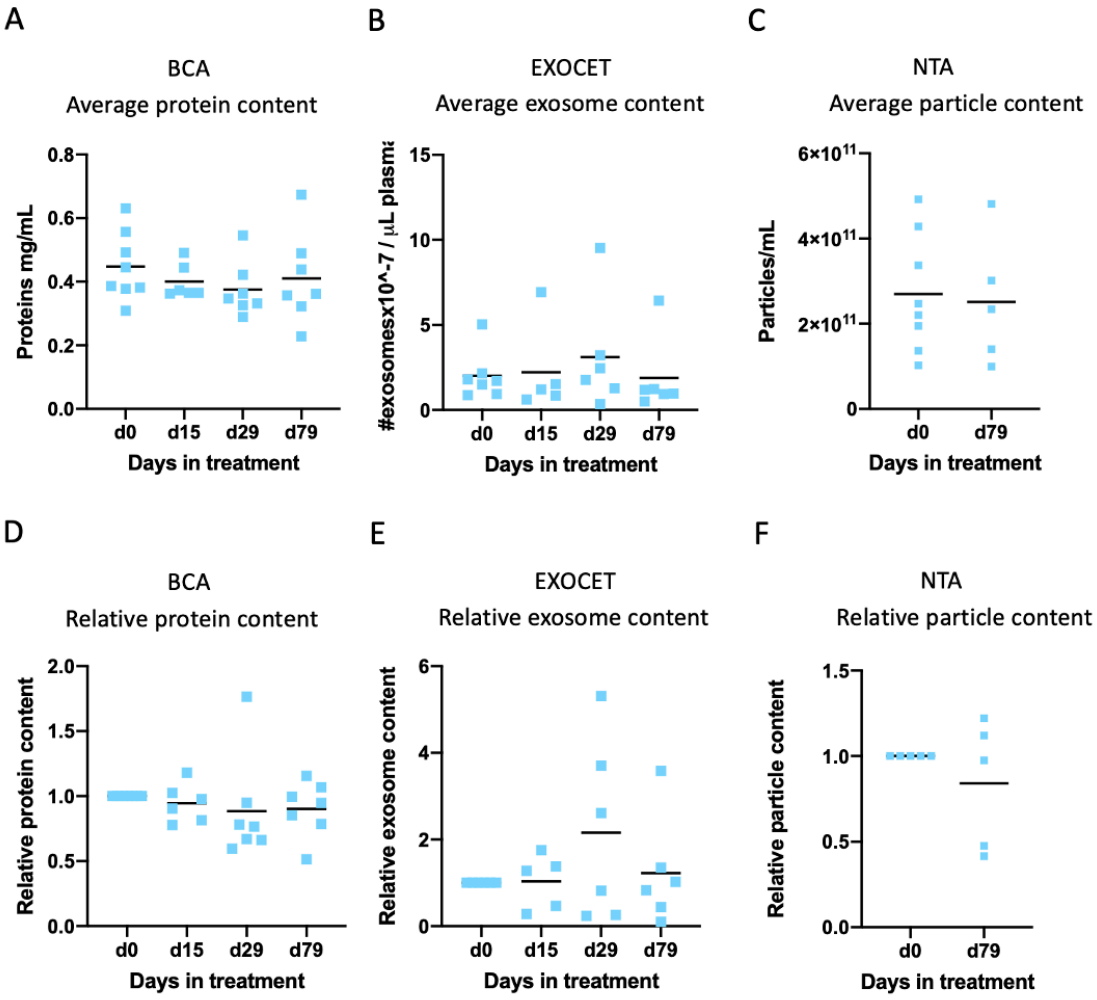

Figure 4.8 EV quantification in ALL patients during the treatment course. Panel A and D show BCA results with protein concentration in ALL day 0 (n=8), day15 (n=6), day 29 (n=7), and day 79 (n=7). Panel B and E represent EXOCET assay in ALL day 0 (n=7), day 15 (n=5), day 29 (n=6) and day 79 (n=6). Panel C and F presents particle content by NTA in ALL day 0 (n=8) and day 79 (n=5). The lower panels D, E and F represents the relative difference between the treatment days compared to the reference value of diagnosis day set as 1. Horizontal bars indicate the mean of each sample group. No statistical difference was detected.

4.3 SCREENING FOR EV BIOMARKERS

Exosomes originating from cancer host cells often contain large amounts of cancer-specific components known to provoke tumor progression and suppress immune responses. It is therefore natural to assume that exosomes originating from leukemic cells will contain a protein signature not found in exosomes derived from healthy cells.

As an approach to screen for EV proteins, we employed a high-throughput proteomics assay based on the combination of SDS-PAGE/Western blotting to separate proteins by size, and a highly multi-plexed antibody array to identify the proteins. The samples were analyzed using a flow cytometer, followed by analysis using a bioinformatics pipeline based on R and Excel commands. One sample from a healthy control, one BCP-ALL patient at diagnosis and one AML patient at diagnosis was supposed to be selected for the analysis, but due to the Covid-19 situation only the BCP-ALL sample was analyzed.

The results from the antibody array analysis is represented in figure 4.9 for the BCP-ALL patient. The original PVDF-membrane was cut into 48 pieces. The x-axis in the diagrams presented in figure 4.9 represents these 48 fractions, from the smallest size in the far left to largest to the right. The y-axis shows the signal strength of the detected protein, measured by Streptavidin-PE binding to the biotinylated protein. The identity of the protein is found by identifying the bead population (with corresponding detection antibody) where the signal stems from. If the antibody is specific, we expect one sharp peak at the expected size of the target protein. The higher the peak the higher abundance of the protein.

A total of 9 proteins were identified among 476 antibody-targets tested. The remaining antibodies showed either too low signals or unspecific peak patterns. High expression of HLA-B, and a low expression of GAPDH and ERK1 was detected. The Apolipoprotein E, part of a larger apolipoprotein family which binds lipids to form lipoproteins, is represented in high amount in several of the fractions. This finding matches our EM images showing abundant lipoproteins in our sample. Another expressed protein was the protein DIABLO (Direct IAP binding protein with low pI), which binds inhibitor of apoptosis proteins (IAPs) and activates apoptosis. The IAP protein Survivin was also detected. PSGL-1, P-selectin glycoprotein ligand-1, was also found to be expressed, as well as a protease inhibitor, alfa$_{-1}$ antitrypsin, and a DNA polymerase delta protein called PCNA (proliferating cell nuclear antigen).

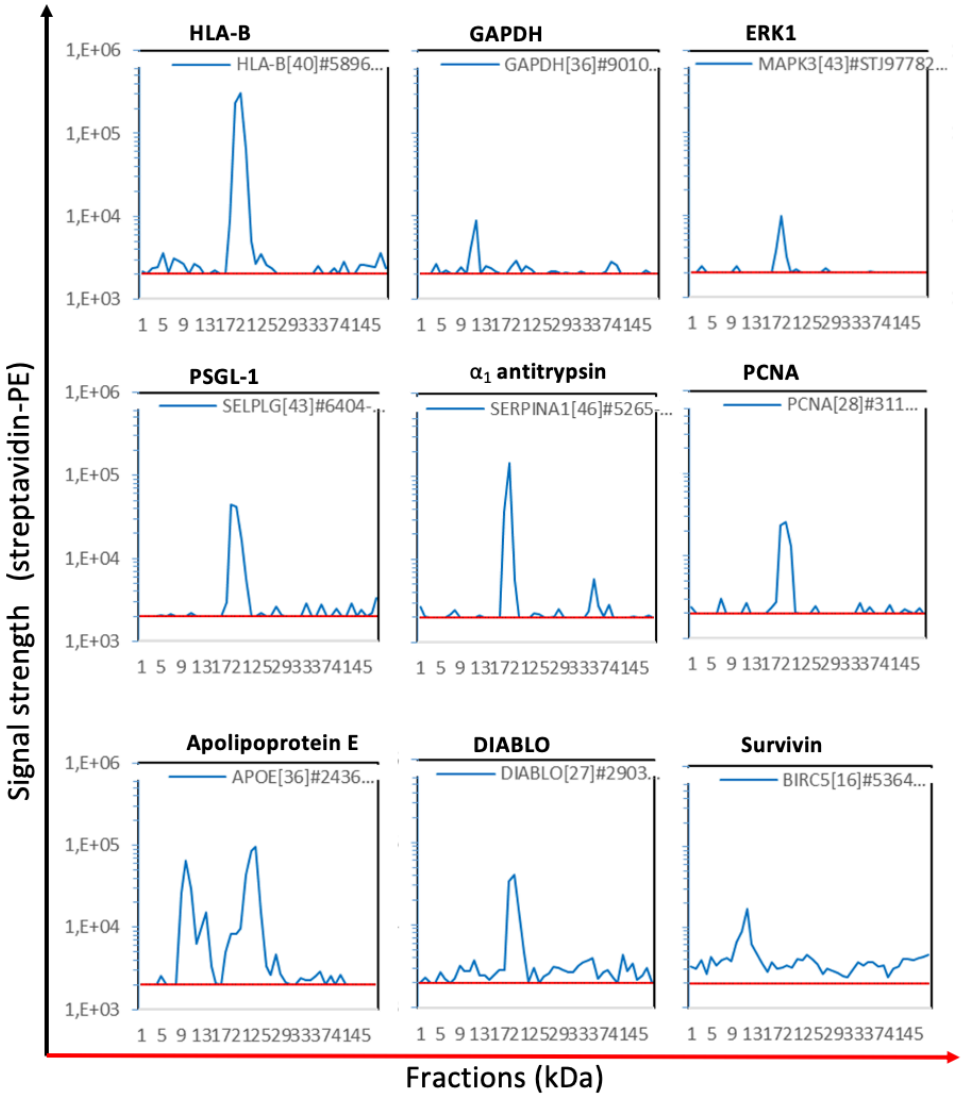

Figure 4.9 Antibody array analysis of exosomal proteins from one BCP-ALL patient. The x-axis shows the protein separations in size (kDa) across 48 fractions, and the y-axis shows the intensity of the signal from each fluorescently bound protein. The higher the peak the higher the concentration of the protein. The gene names are indicated inside the graph, with the corresponding protein names above each graph.

We next sought to verify the findings from the above proteomics screen by using Western blotting to test all our samples. The western blots were also analyzed using ImageJ software, in order to get a relative quantification of the signal strength in each band for comparative purpose. As we were unable to do an extensive verification due to economic reasons, we chose to verify the expression of Survivin and α1-antitrypsin as these are proteins known to have higher serum concentration in other cancer types and identified as possible biomarkers for various cancers (36, 37).

Figure 4.10 shows the results from the western blotting and relative quantification with Survivin (panel A and B) and α_1-antitrypsin (panel C and D). It seems like both proteins are expressed at varying levels in all samples, both in patients and in controls, with some individuals having stronger expression than others. Panel B (Survivin) and D (α1-antitrypsin) indicates no significant difference between patient groups compared to the controls.

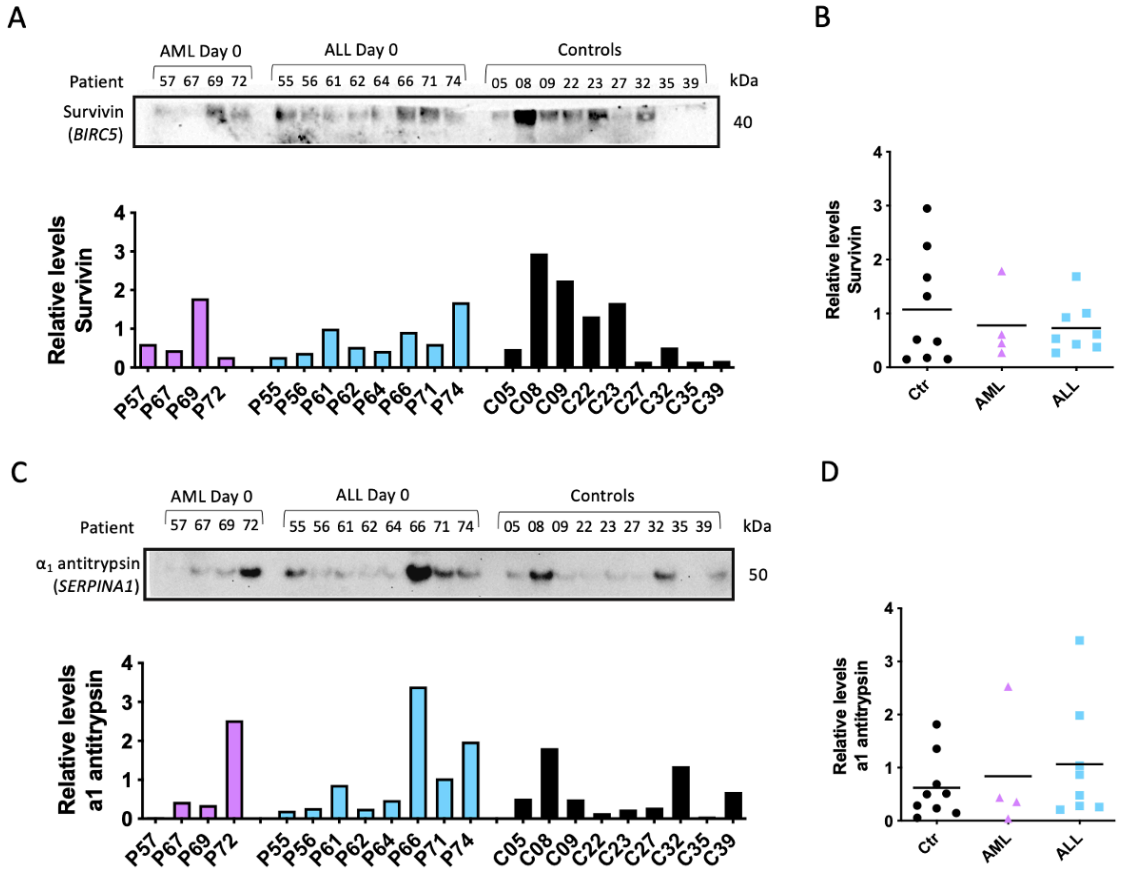

Figure 4.10 Western blot analysis of Survivin and a_1 antitrypsin in patients at diagnosis. A) Western blot and corresponding relative expression levels of Survivin normalized against protein concentration (BCA) in exosome isolates from patients at diagnosis and in controls. B) Compilations of quantifications done in panel A. Bars indicates the mean of each sample group, and no significant difference C) Western blot and corresponding relative expression levels of α_1-antitrypsin normalized against protein concentration (BCA) in exosome isolates from patients at diagnosis and in controls. D) Compilations of quantifications done in panel A. Bars indicates the mean of each sample group, and no significant difference. Black dots: controls. Purple dots: AML patients. Blue dots: ALL patients

We next investigated whether the expression of survivin, α_1 antitrypsin and PSGL-1 would change during the course of treatment. This was tested using a western blot for the BCP-ALL samples as there was not enough samples from the AML timeline.

The results are depicted in figure 4.11 and show no indication of statistical difference in relative expression levels during treatment. Both survivin (panel A) and PSGL-1 (panel E) seem to have a relative equal amount through each treatment day, with survivin being weakly expressed and PSGL-1 highly expressed. For a_1 antitrypsin (panel C) on the other hand there seems to be more of a varying expression between the patients. Panel B, D and F shows that none of the proteins have any significant difference in protein expression between the treatment days.

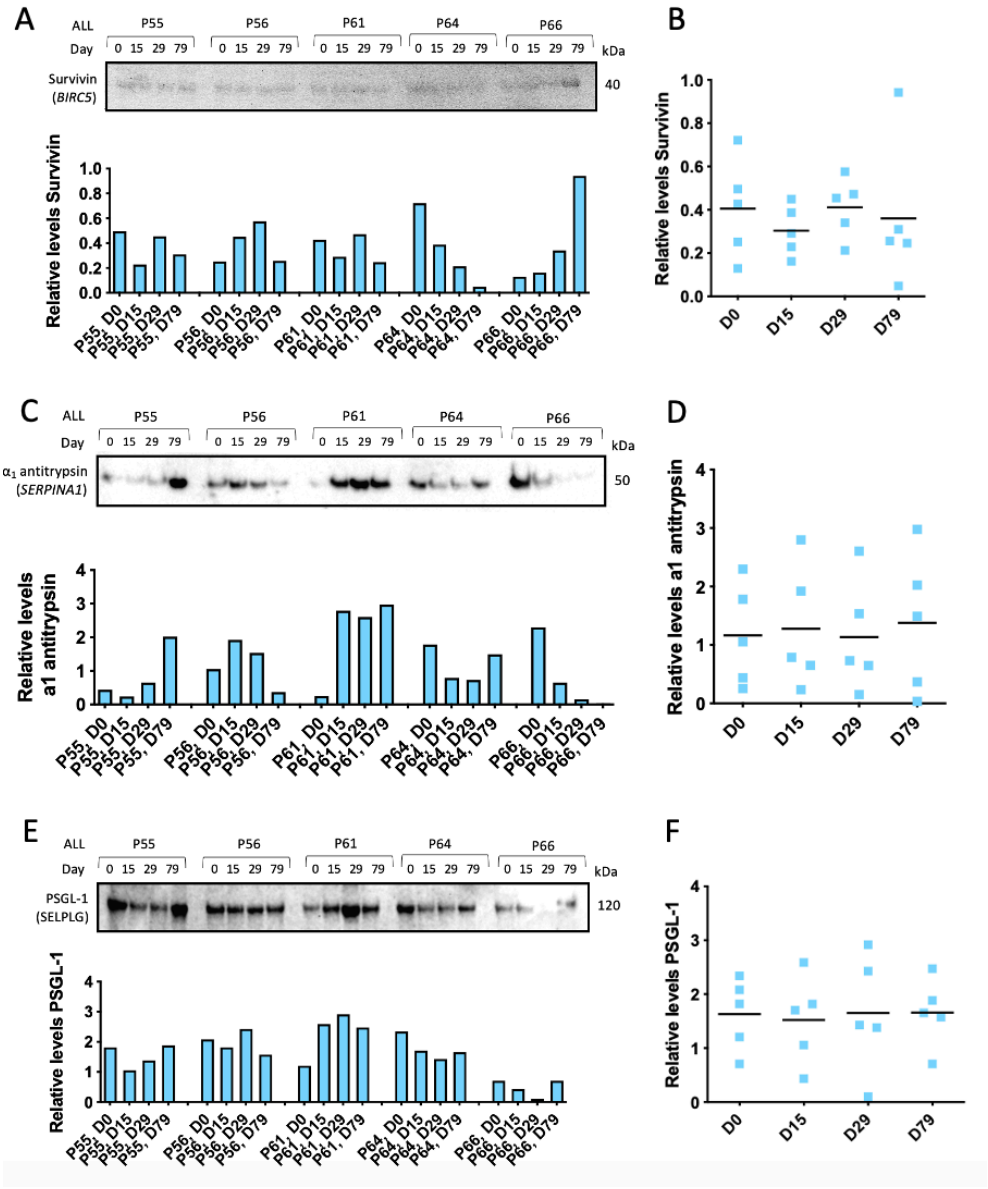

Figure 4.11 Western blot analysis of survivin, α_1-antitrypsin, and PSGL-1 in exosomes during the course of treatment. A) Western blot analysis of Survivin and normalization by ImageJ. B) Compiled data of relative Survivin expression from the different time points. C) Western blot analysis of α_1-antitrypsin and normalization by ImageJ. D) Compiled data of relative a_1 antitrypsin expression from the different time points. E) Western blot analysis of PSGL-1 and normalization by ImageJ. F) Compiled data of relative PSGL1- expression from the different time points. The horizontal bar represents the mean of each group. No statistical difference detected.

5 DISCUSSION

5.1 METHODOLOGICAL CONSIDERATIONS

5.1.1 PATIENT SAMPLES

In this study, we utilized plasma samples from pediatric acute leukemia patients. These samples had already been collected and biobanked in connection with a PhD project before this study started where a total of 76 children were included. The samples included in the present study had some limitations. Firstly, plasma biobanking started quite late in the PhD project, from patient 55 and onwards, meaning there was only a limited number of samples to choose from. Secondly, both T-ALL and AML are rare diseases with only 1-2 and 3-4 new cases in Norway each year, respectively. Meaning we had less material from these patient groups compared to BCP-ALL, which have more than 20 new cases each year and is therefore the majority of our samples. Thirdly, when we chose to streamline and speed up the exosomal isolation process with the exosome isolation kit, we had to select a limited number of samples as the kit could only take 48 isolations. This limited our patient and control amounts, which then had to be divided between the different patient groups and healthy controls. As we had more plasma samples from BCP-ALL and we also questioned how the exosomal levels would change during treatment it was natural to have the majority of our samples from this patient group.

When analyzing the results, it is therefore important to underscore that there is one T-ALL (P71) in the ALL patient group and to get a clearer picture of AML we would need more samples. It would in any case have been preferable to have more samples as large individual differences is to be expected.

5.1.2 EXOSOME ISOLATION

Since exosomes became a case of interest, their purification and isolation have been subject to constant debate. Not only is their small size a major issue, but isolation from plasma greatly increases the difficulty. Plasma contains larger vesicles like apoptotic bodies and microvesicles, as well as large proteins, immune complexes, and lipoproteins. For this reason, there is no

standardized method for isolating exosomes from plasma without co-isolating unwanted impurities.

For the two methods chosen in this thesis, we have emphasized isolation of small EVs with less protein and lipids. However, there is no currently used isolation protocols that discriminate between different EVs of similar size, meaning separating exosomes from other small and medium sized vesicles needs further protocol development.

During the first part of the project, when utilizing ImageStream, the exosomes were isolated through size-exclusion chromatography combined with differential up-stream centrifugation and filtration (200 nm). This was an already established protocol known to minimize impurities and reducing the complexity of the plasma sample (38). The technique separated exosomes from other non-EV components and purified exosomes was found in fractions 3-5. This method was not without its drawbacks, and other than being said to yield a low vesicle count in other reports (39) it was a very tedious process. The column required a lot of time to prepare, including running samples and washing. Another concern was the columns expiry date, as each sample should run on the same column to yield the same results. When a column is washed with ethanol and stored in 4°C this increased the risk of a bacterial buildup between each isolation procedure.

When the ImageStream machine broke down we decided to choose a faster and more consistent method of exosome isolation. The Exo-spin™ exosome isolation kit combines the SEC technique with precipitation. This was a simpler and quicker way to enrich for exosomes, and also provided a streamlined system to avoid varying preparation steps like different collection tubes, storage temperatures, freeze thaw cycles etc. The kit is said to yield a higher concentration and give a superior separation, but we did not directly compare the two methods. At this point in the process it was more important to have a reproducible and consistent way of handling all the samples.

Another concern was working with frozen samples of exosomes and if it had any effects on the exosome integrity and content. There are no criteria for biobanking enriched exosomes from plasma and we have no way of knowing if the samples are affected by continuous freezing and thawing. Over time the samples may or may not have exosome aggregations, bacterial build-up and/or other flaws.

5.1.3 IMAGESTREAM SUBSET SPECIFIC ANALYSIS

The original project was to detect and characterize specific EV subsets, exosomes in particular, and further quantifying them using ImageStream. Unfortunately, the machine broke down and this was not accomplished.

During this part of the study, the exosomal samples (obtained from SEC) were fluorescently stained with the lipid-penetrable dye CFDA-SE that is converted to CFSE as a consequence of ester hydrolysis. This was a way of distinguishing between vesicles and other lipid components present in plasma. However, before we stained with CFDA-SE we tested another fluorescent compound called Calcein AM. The Calcein AM dye is cleaved to fluorescent calcein by esterases and works in the same manner as CFDA-SE.

When we still had a working ISx we did have some difficulty with a phenomenon called swarm that appeared after using the instrument a while. This means our samples seemed to contain a lot of debris that did not contain exosomal markers. We did suspected aggregations in our samples but making fresh samples did not solve this problem. We initially thought it could be the calcein dye causing unspecific labeling, but we got the same results when changing to CFDA-SE. We speculated that the swarm could be due to insufficient dilutions, causing a high concentration that would cause random detection from the ISx. However, several dilutions were tested, and the swarm effect was still evident. We found a paper on sEV characterization using flow cytometry and they had found that the majority of their circulating particles were lipoproteins, as they are within the size range of sEVs but lacked the common markers (18). Considering the EM pictures (figure 4.3), it is evident that lipo-particles are a major constituent of our samples.

If we were able to create a gating strategy to characterize for spesific exosomes the next step would have been to test unprocessed plasma samples and eliminating the impacts of the different isolation methods.

EXOSOME IDENTIFICATION

There are no current methods for separating exosomes from other small EVs, and we expect our samples to contain a heterogenous population of small EVs. The original plan was to establish a gating strategy using different exosomal and leukocyte markers utilizing the ImageStream and aiming to classify subsets of exosomes originating from different leukocyte populations. Without this technique we decided one of the ways to verify exosomal content

in our samples was through western blotting combined with NTA and EM as these are cornerstone methods for exosome verification.

5.1.4 MEASURING EXOSOMAL CONCENTRATION

As mentioned, the original project was to utilize the ImageStream machine to first classify the subsets of different EVs in our samples and then quantify and compare healthy controls vs. patients. We expected our samples to contain a heterogenous population of EVs, and without the ISx method enumeration of bona-fide exosomes is challenging. We chose to tackle this assessment through three different methods; BCA, NTA and EXOCET giving us the sample concentration of proteins, particles and exosomes, respectively. In addition, we sent one sample for EM to verify presence of structures with morphology of exosomes. However, none of these methods would give us any accurate profiling of particular subsets of EVs.

There are merits and drawbacks in each of the three methods, but the one most commonly used to quantitate EVs is the nanoparticle tracking analysis machine. NTA uses light scattering measurements to determine particle concentration as well as size and size distribution (10 - 1000 nm) in a relatively rapid manner. It compensates variables in a sample and increases precision by enabling replicated video measurements, which we chose to be 3 measurements á 60 sec. NTA has a general accuracy within 5% of particle size as long as appropriate hardware and software settings are applied (40). Errors known to occur often varies between the instruments and different software. These are normally inaccurate viscosity assessments, incorrect temperature measurements, and external vibrations, which were corrected by the default settings in the newest software (NTA 3.4). We also used the largest instrument NS500 which has a computer-controlled camera, automated sample induction and handling, which decreases errors which normally occur on the smaller machines (41). It is a criticism of NTA that it lacks standardization as variability between instruments with different specifications gives different data and is therefore not transferrable.

Before each measurement the machine is calibrated with size-standard beads. For our experiments we used polystyrene beads, however there are reports reporting that polystyrene beads have a 4 times higher light scatter than EVs of same size (41). This is due to their reported difference in refractive index, approx. 1.59 for polystyrene and 1.39 for EVs. This could lead to an inaccuracy in EV concentration measurements and researchers in the field recommend silica beads (index of 1.45) instead (41).

Another drawback when using this technique is the machine's inability to distinguish between vesicles and non-vesicular debris. Meaning, if we have co-isolated lipoprotein particles, which are the same size as most EVs and in high excess in blood plasma, this would give false positive results. When utilizing the NTA we had a limited amount of time allocated (one full day), which is the reason for not having all the 48 samples tested.

Both the BCA and the EXOCET assays utilizes colorimetric detection as a readout. This in itself is a widely used method due to low cost, simple operation and quick response making it suitable for replication. Here it is important to work within the linear range of the assay and ideally use standards similar to the substance of interest.

For the protein quantification assay we assumed a higher protein count would represent a higher EV count from our enriched samples. The BSA standard is tested to be one of the most reliable proteins when analyzing EV samples (42). The EXOCET assay measures the activity of esterases known to be withheld inside exosomes, and the readout is measured against a standard curve consisting of samples with known concentrations of exosomes provided by the manufacturer. For the EXOCET assay we had to limit our number of samples to 40 out of the 48 isolated samples due to constraints in the setup. A total 96 wells were available with the kit in total, 16 wells were used as standards, leaving us with 80 wells for samples. As samples were run in duplicates, this limited our analysis to 40 samples.

As mentioned, since there is no current standard for quantifying EVs the results from the above methods will only have an approximation of enumerating EVs in our samples and does not provide an exact quantitative profile. It is also expected that the different methods will give varying results, not only because of the obvious differences in what content we are measuring, but also variations in the specific techniques.

5.1.5 BIOMARKER ASSAY

To screen for potential protein-biomarkers in the patient EV sample, we utilized a high-throughput proteomics approach combining SDS-PAGE/Western blotting for size separation and multiplexed antibody array to identify the proteins.

Due to the complexity of the technique, we planned to analyze one sample from a healthy control, one sample from a BCP-ALL patient at diagnosis, and one sample from an AML patient

at diagnosis. Unfortunately, because of the current COVID-19 pandemic situation we were forced to abandon further analysis, and only one BCP-ALL sample was screened. It was therefore impossible to directly compare the data from the screen to a healthy control. Also, in our screen, we only used an antibody array towards proteins <50 kDa. Screening using an antibody array towards proteins >50 kDa was also planned but had to be abandoned.

5.2 FINDINGS

5.2.1 CHARACTERIZATION OF SMALL EVS IN PEDIATRIC PATIENTS

DETERMINATION OF EXOSOMAL SIZE AND MORPHOLOGY

Particle size was assessed using NTA and Figure 4.2A confirms that we had particles of small EV size in our samples (mode 130-150nm). However, not all of the isolated particles fell into the size range of exosomes (40 - 150 nm). The larger sized particles may be non-exosomal vesicles of different sizes and/or aggregates of lipoproteins or small EVs. This was expected as we assume our samples contain a heterogenous population of EVs. Size distribution curves showed a percentage of the particles being over 200 nm, which should not occur as the plasma samples were processed through a 0.2 μm filter, and the SEC-column had a 200nm cut-off. This therefore likely represent lipoprotein- or small EV-aggregates. Previous studies have reported similar results when isolating exosomes from plasma using precipitation-based reagents: particles of non-exosomal size were identified by NTA, and EM verified the structures as exosome-like aggregates (43-45). In support of particle aggregation, is our EM analysis, showing aggregates of both vesicles and lipoproteins (Figure 4.3). Our NTA results (Figure 4.2) also show a lower mean size for the controls (130 nm) compared to the patient groups (150 nm). The larger particle size could represent apoptotic bodies and other cell debris potentially being in higher amount in blood of patients. Interestingly, the two high-risk patients in our study group, AML P57 and ALL P71, both had the highest mode size (180-190 nm) compared to the other samples.

DETECTION OF EXOSOMAL MARKERS

The tetraspanin proteins CD63 and CD81, among others, have been used as standard exosomal markers (13, 15) . We probed for CD63 and CD81 using Western blotting to verify our exosomal content (Figure 4.4). Similar to previous publications we were able to detect their

expression in our samples. For the healthy controls and the ALL patients we confirmed expression in all the samples, but for the AML patients they were not detected in all samples. The signals for both markers were overall weak.

The ALL data in figure 4.4 shows an interesting tendency towards higher CD81 expression at diagnosis, which is then replaced by a higher amount of CD63 at day 79 in the treatment protocol. Previous studies using CD63 and CD81 show varying similarities, and there are different reports about the expression profile of tetraspanins in B cells. In one study exosomes released by four different B-cell lymphoma cell lines were investigated, and these were found to completely lack CD9, and one of the lymphoma cell-lines (SUDHL-6) lacked CD63. All four cell lines expressed CD81. In contrast, their positive control, which was exosomes derived from a colorectal cancer cell line (SW480), had low expression of CD81 and high expression of CD63 (19). Another report showed no CD63 expression in exosomes derived from primary B cells, but strong expression of CD81 (46). This data could collectively indicate that B cells release exosomes with low or no CD63. This is in contrast to exosomes analyzed from a wide range of other tumor cell lines, where CD63 appears to be commonly expressed (47). When comparing with the AML, and T-ALL (P71) in figure 4.4, which both show expression of CD63 at diagnosis, we speculate that patients with ALL have high amounts of B-cell derived exosomes at diagnosis and therefor show little expression of CD63. In contrast to day 79 after treatment where the patient plasma should have less B-cell derived exosomes and therefor more expression of CD63 from healthy-cell exosomes.

LINEAGE SPECIFIC SURFACE MARKERS

We further tested expression of markers commonly expressed by BCP-ALL (CD19) and AML (CD34) blasts. CD34 may also be over-expressed on ALL blasts. These markers were tested by Western blotting (Figure 4.5). Classifying exosomes based on parental-cell markers have been proven to be difficult due to exosomal heterogeneity (13, 22). However, some studies have been able to identify the presence of LAAs in the exosome cargo.

Figure 4.5A showed CD19 being highly expressed in all samples, but more in ALL compared to the controls, this is seen in the relative amounts in figure 4.5B having a statistically significant difference ($p = 0.02$). These results indicate that we have B-cell derived exosomes in all our samples, more in BCP-ALL than in AML and controls. Several components of B-cell surface antigens have already been detected in exosomes from different B-cell lymphoma cell lines

(19). However, other common leukocyte antigens like CD45 was not found on the B-cell lymphoma derived exosomes, even though they were widely expressed in the host cells (19). This underscores the heterogeneity of the disease as well as of exosomal subsets and the difficulty in classifying exosomes based on parental-cell markers (13, 22).

In figure 4.5C the hematopoietic stem cell marker CD34 had an uneven expression between the samples with more in the patient groups than the controls. Figure 4.5D shows there being a statistical significance ($p = 0.006$) between ALL and the controls. For the AML, although a small test group, CD34 was expressed higher than in the control group. This correlates with previous studies were exosomes isolated from AML patients (adult) expressed myeloid markers, among others CD34, but also here the expression differed between the test subjects (48).

5.2.2 QUANTIFICATION OF EXOSOMES

As mentioned, cancer cells have been found to be avid exosome producers and determining whether the patient groups had a higher exosomal plasma content than healthy controls was one of the main goals in this study. We quantified the exosomal content from our samples by the three different methods, NTA, BCA, and EXOCET, and compared patients at diagnosis with healthy controls.

The NTA analysis in figure 4.6C showed that both AML and ALL patients had a higher particle content per mL than the healthy controls ($p<0.05$). This was also evident during testing, as the patient samples had to be extensively diluted to stay within the recommended detection levels ($1x10^8$ particles/mL) unlike the healthy controls. These data were partly confirmed by measuring protein concentration using the BCA assay in figure 4.6A, where we found that the ALL isolates had a higher protein concentration than the healthy controls ($P = 0.0155$). The AML on the other hand had no statistical difference with the controls in the BCA assay. In contrast, quantification by the EXOCET assay (Figure 4.6B) did not reveal any differences between the groups. Both the BCA and the NTA suggests an increase in protein and particle content between ALL and healthy controls (Figure 4.6 A and C).

From a study testing if exosomes from plasma could be used in predicting therapeutic response in adult AML, it was stated that newly diagnosed adult patients had considerably higher levels of plasma exosomes compared to normal controls (32). They had based their study on findings

from patients with melanomas and other solid tumors reporting to have a high level of protein from isolated plasma exosomes reflecting their disease burden. This study used ultracentrifugation and SEC to isolate their exosomes and analyzed their fractions by measuring protein concentration. They measured an average of 55.2 µg protein/mL plasma in AML and 13.1 µg protein/mL plasma in normal controls. Compared to our results of ALL average 447 µg protein/mL, AML 389 µg protein/mL and healthy controls 296 µg protein/mL. The difference may due to different isolation techniques and different protein measuring techniques. They also had a much higher yield from NTA, showing an average of 5 x 10^{13} particles/mL plasma compared to our AML samples yielding an average of 1.3 x 10^{11} particles/mL for AML and 2.7 x 10^{11} particles/mL for ALL, 4.5 x 10^{10} for the controls (32).

Another study done on plasma derived exosomes in acute myeloid leukemia they stated an increased exosomal load in plasma of newly diagnosed adult AML patients. This was found to correlate with a higher risk of relapse and patients in complete remission were shown to have low exosomal levels parallel to that of healthy controls (27). They had also relied their quantification on protein content from SEC fractions isolated from plasma. We have found our data (Figure 4.6) to correlate to some extent to the already existing data on the matter. The BCA shows increased protein concentration in our ALL compared to healthy controls. We also found both our patient groups to have a higher particle content than the healthy controls. This suggest a pattern of higher content of EVs in the patient groups, but which subtype of vesicles is unknow. It has been reported that exosomes accumulated in the plasma of cancer patients can act as surrogates for tumor cells (32). This may not be the case for hematopoietic cancers were the malignancy acts more as a liquid tumor. It may be a correlation between the denser the leukemic blasts are in the blood, the more exosomes or other EVs we will find. It is also important to remember that both BCA and NTA could have measured other impurities as we did find lipoproteins in our sample by TEM (Figure 4.3).

Due to the different performances of the methods, we directly compared the three methods against each other. The data in figure 4.7A showed EXOCET and BCA having a tendency ($p=0.08$) towards correlation, while the NTA assay (Figure 4.7 B and C) did not correlate to either of the two other methods. This could be related to the nature of the two methods as NTA is biophysical and the two others biochemical. Not only do they differ in chemical and physical properties, but the techniques also vary in procedure steps that may affect the results. As the

two biochemical methods does not give us any visual of what we are actually measuring it is easier to comprehend the NTA data. The NTA data also shows similar particle concentrations measured from exosome isolates as other groups have reported (44).

CHANGE IN EXOSOMAL CONTENT DURING TREATMENT

To test if the exosome content would change during treatment, we quantified our exosome fractions from the BCP-ALL patients, which was the only samples we had a clear timeline on. Figure 4.8 A, B and C shows the analysis done by the three quantifying methods BCA, EXOCET and NTA, respectfully. From day of diagnosis (d0), through induction phase (d15 and d29) and treatment (d79) there was no statistically significance found in any of the methods. Panel D, E and F showed there was no relative difference between the treatment days when the reference value of day 0 was set as 1. All patients in the BCP-ALL group were all standard risk or intermediate risk, and it would have been interesting if we could have included some high-risk patients, or patients that have progressed into relapse. No relapse has been reported for the included ALL samples until now, and we could thus not with this project assess whether exosomes could predict relapse.

5.2.3 SCREENING FOR BIOMARKERS IN BCP-ALL

Since exosomes from cancer cells are known to contain cancer-specific proteins we screened for such signature proteins in one BCP-ALL patient at diagnosis. An antibody array was employed and the result (Figure 4.9) showed the EV isolate expressed 9 different proteins; HLA-B, GAPDH, ERK1, Apolipoprotein E, Diablo, PCNA, P-selectin, α1-antitrypsin and Survivin. To verify our findings, we utilized western blot to test all our samples for expression of α1-antitrypsin and survivin as they are known to be overexpressed in other cancers (Figure 4.10). We also used western blot to see if this expression would change during treatment of the ALL patients (Figure 4.11). Below follows a discussion of the detected markers with regards to relevance for BCP-ALL.

HLA-B: This is the human leukocyte antigen B protein which is part of the three main MHC class I genes in humans. HLA-B is therefore present on almost all human cells and is consequently known to be expressed on exosomes (20, 22). As part of our initial western blot characterization, we blotted for MHC class I using an antibody recognizing HLA-A/B/C

without any results, thus this find most likely tells us that something did not work during the immunostaining.

GAPDH: Glyceraldehyde 3-phosphate dehydrogenase is a well-known housekeeping gene, which is responsible for catalyzing the sixth step of glycolysis. As we do not expect any EVs to perform glycolysis, it is more likely that GAPDH has other functions. Recent reports have found GAPDH to play a part in activation of apoptosis and membrane trafficking (49, 50), but more importantly GAPDH has newly been discovered to be required for exosomal biogenesis, both in assembly and secretion (51) .

ERK1: Extracellular signal-regulated kinase-1, is a known housekeeping gene that mediates functions such as cell growth, survival and differentiation (52). ERK1 is therefore a potential oncogene and is found to be released in EVs from different cancer cell lines (53). ERK1 is also found to be upregulated 2 - 4.5-fold when cells were short-term incubated with exosomes and the same study found that exosome uptake through lipid-raft mediated endocytosis was dependent on the ERK1 pathway (54). Future studies should explore the possibility of EVs carrying these proteins to help internalize in recipient cells.

APOLIPOPROTEIN E: The Apolipoprotein E is part of a larger apolipoprotein family that binds lipids to form lipoproteins. Lipoproteins, which are single layered phospholipid vesicles, carry hydrophobic molecules in blood or other extracellular fluids (55). Apolipoprotein E is a major component in many different lipoproteins and these finding is in line with our EM images showing abundant lipoprotein complexes (figure 4.3).

DIABLO: Direct IAP binding protein with low pI binds inhibitor of apoptosis proteins (IAPs) and consequently activates apoptosis (56). Diablo is implicated in a broad spectrum of cancers because of this apoptotic function (56). A study on Diablo expression levels done on 60 adult AML patients receiving therapy, found the expression levels to be an important predictive factor. The expression levels were assessed at diagnosis and initially low values correlated to negative outcome like chemoresistance (57). It would be interesting to see if other patients in our study had shown any difference in Diablo expression and correlated the results with risk factors and overall survival.

PCNA: Proliferating cell nuclear antigen is a DNA polymerase delta protein involved with eukaryotic DNA replication (58). Many studies show that different cancer types express high levels of PCNA (59). It is found that membrane associated PCNA acts as a ligand for the innate immune receptor NKp44 and when this interaction is inhibited in various human cancer cell lines, the cancer cells viability decreases (59). PCNA is also found to be expressed on the surface of prostate cancer cell line DU145 were it binds to NK cells (via the NKp44 receptor) to inhibit their cytotoxicity (60). The fact that we found this protein in our EV fraction could indicate that we have exosomes derived from cancer cells that carry this protein as an overall protection against the innate immune system.

ALFA-1 ANTITRYPSIN: Alfa-1 antitrypsin inhibits various proteases released from inflammatory cells (61). Alfa-1 antitrypsin is normally released in a steady state manner, but in response to infection it is released at higher levels (36). When screening our samples for Alfa-1 antitrypsin by Western blotting (Figure 4.10C), we found the protein to be variably expressed. Even though Alfa-1 antitrypsin is expected to be co-isolated in our samples as it is known to be abundant in plasma, it is natural to assume that the patients expressing higher levels of the protein are also under an immune induced response. Furthermore, as researchers have found consistent evidence of Alfa-1 antitrypsin having antitumor effects (36), it is interesting to see that the AML High Risk patient 57, had no expression of Alfa-1 antitrypsin (this patient did not express CD63 or CD81 either). However, both P71 (HR) and 74 (IR) had high expression, so clearly more data is needed to draw any conclusions.

When looking at the ALL treatment timeline in figure 4.11C there is also a difference between the expression levels of Alfa-1 antitrypsin. For example, patient 66 showed high amounts at diagnosis, but went over to a steady state during treatment, which may indicate good treatment response. Unlike patient 55 which had a relative high expression at diagnosis compared to the other groups but had an even higher concentration after 79 days in treatment. They were both SR grouped.

SURVIVIN: Survivin is a member if the IAP family and stops programmed cell death by inhibiting caspase activation and is known to be highly expressed in tumor cells and fetal tissue. It is also shown that tumors having an overexpression of Survivin is associated with poor prognosis (37). Furthermore, EVs extracted from plasma of breast cancer and prostate cancer patients were both found to be highly enriched in Survivin (62, 63). All the test groups, AML,

ALL and healthy controls (Figure 4.10A) expressed a various amount of this protein, and although we did not detect a significant difference in expression of Survivin in patient exosomes, it would be interesting to test a larger cohort of patients.

PSGL-1: PSGL-1 is expressed on the surface of hematopoietic stem cells, and works as a adhesion receptor responsible for recruitment, rolling or anchoring of leukocytes to the bone marrow, lymph or sites of inflammation (64). One study on MVs´ role as messengers during pregnancy found that the MVs bind to T-lymphocytes through PSGL-1 (65). Another study found PSLG-1 to act as a negative regulator for T-cell function in viral and tumor mice models (66). Finding PSGL-1 in our EV isolate may suggest that we have exosomes or MVs derived from cancerous cells carrying this adhesion receptor in a) aim of anchoring to endothelial cells and transferring its cargo b) in aim to exhaust T-cell response.

5.3 CONCLUSION

In this thesis, we aimed to test whether exosome quantification and/or phenotype could be used as biomarkers for acute leukemia in children. The long-term goal would be to assess whether exosome characteristics could be used to predict risk of relapse, but this was beyond the scope of this thesis. We demonstrate here the successful isolation of EVs and exosomes from plasma of pediatric acute leukemia patients and show higher abundance of EVs in the patients compared to controls when assessed by NTA analysis at particle level and by a higher protein concentration (BCA assay). This is in line with current literature for other cancers, and further analysis should be done on a larger cohort of patients. Presence of exosomes in our isolates was verified by electron microscopy. Further, we found variable expression of the exosomal markers CD81 and CD63 in patient exosomes and conclude that exosomes from BCP-ALL patients may not express CD63 at the same level as other cells. Thus, CD63 is a potential negative marker for B-cell derived exosomes in BCP-ALL patients at diagnosis. Finally, we found expression of 9 proteins in our EV isolate by an antibody array screening approach, where a few of them have the potential to be further analyzed as possible biomarkers.

5.4 FUTURE PERSPECTIVES

An imminent goal would be to develop a better and preferably standardized method for isolation of exosomes from plasma. Alternatively finding a way of utilizing unprocessed samples to

bypass the burden of the separation procedures. Inadequate isolation methods and lack of standard techniques differing between laboratories limits the accuracy and reproducibility of exosomes or EVs as biomarkers in a clinical setting.

Another challenge in the exosome field is the lack of reliable markers for validation of exosomes that distinguishes them from other subsets of EVs. Establishing a standardization of verified markers to identify exosomes and other vesicle types is therefore needed, which could be accomplished using the screening approach presented in this thesis.

We would also as a next step include a larger amount of patient samples to verify our findings of an increased exosomal load at diagnosis both for ALL and AML. In addition, more Western blots should be done to verify the low levels of CD63 at diagnosis in the BCP-ALL patient group, and it would be interesting to study why CD63 apparently is expressed at low levels in B cells.

REFERENCES

1. Lanzkowsky P, Lipton JM, Fish JD. Lanzkowsky's manual of pediatric hematology and oncology: Academic Press; 2016.
2. Kolmannskog S, Flaegstad T, Helgestad J, Hellebostad M, Zeller B, Glomstein A. [Childhood acute lymphoblastic leukemia in Norway 1992-2000]. TidsskrNor Laegeforen. 2007;127(11):1493-5.
3. Boyd SD, Arber DA. CHAPTER 18 - Acute myeloid leukemias. In: Porwit A, McCullough J, Erber WN, editors. Blood and Bone Marrow Pathology (Second Edition). Edinburgh: Churchill Livingstone; 2011. p. 273-88.
4. Gaynon PS. Childhood acute lymphoblastic leukaemia and relapse. British journal of haematology. 2005;131(5):579-87.
5. Pui C-H, Robison LL, Look AT. Acute lymphoblastic leukaemia. The Lancet. 2008;371(9617):1030-43.
6. Schmiegelow K, Forestier E, Hellebostad M, Heyman M, Kristinsson J, Söderhäll S, et al. Long-term results of NOPHO ALL-92 and ALL-2000 studies of childhood acute lymphoblastic leukemia. Leukemia. 2010;24(2):345-54.
7. Inaba H, Greaves M, Mullighan CG. Acute lymphoblastic leukaemia. The Lancet. 2013;381(9881):1943-55.
8. Karlsson L, Forestier E, Hasle H, Jahnukainen K, Jonsson OG, Lausen B, et al. Outcome after intensive reinduction therapy and allogeneic stem cell transplant in paediatric relapsed acute myeloid leukaemia. Br J Haematol. 2017;178(4):592-602.
9. Abrahamsson J, Forestier E, Heldrup J, Jahnukainen K, Jonsson OG, Lausen B, et al. Response-guided induction therapy in pediatric acute myeloid leukemia with excellent remission rate. J Clin Oncol. 2011;29(3):310-5.
10. Johnson SM, Dempsey C, Parker C, Mironov A, Bradley H, Saha V. Acute lymphoblastic leukaemia cells produce large extracellular vesicles containing organelles and an active cytoskeleton. Journal of extracellular vesicles. 2017;6(1):1294339.
11. Porwit A, Béné MC. CHAPTER 19 - Acute lymphoblastic leukemia/lymphoma and mixed phenotype acute leukemias. In: Porwit A, McCullough J, Erber WN, editors. Blood and Bone Marrow Pathology (Second Edition). Edinburgh: Churchill Livingstone; 2011. p. 289-301.
12. Raposo G, Stoorvogel W. Extracellular vesicles: exosomes, microvesicles, and friends. J Cell Biol. 2013;200(4):373-83.
13. Mastoridis S, Bertolino GM, Whitehouse G, Dazzi F, Sanchez Fueyo A, Martinez-Llordella MJFiI. Multiparametric analysis of circulating exosomes and other small extracellular vesicles by advanced imaging flow cytometry. 2018;9:1583.
14. Jeppesen DK, Fenix AM, Franklin JL, Higginbotham JN, Zhang Q, Zimmerman LJ, et al. Reassessment of exosome composition. Cell. 2019;177(2):428-45. e18.
15. Kowal J, Tkach M, Théry C. Biogenesis and secretion of exosomes. Current opinion in cell biology. 2014;29:116-25.
16. Andreu Z, Yáñez-Mó M. Tetraspanins in extracellular vesicle formation and function. Frontiers in immunology. 2014;5:442.
17. Palmirotta R, Lovero D, Cafforio P, Felici C, Mannavola F, Pellè E, et al. Liquid biopsy of cancer: a multimodal diagnostic tool in clinical oncology. Therapeutic advances in medical oncology. 2018;10:1758835918794630.

18. Sódar BW, Kittel Á, Pálóczi K, Vukman KV, Osteikoetxea X, Szabó-Taylor K, et al. Low-density lipoprotein mimics blood plasma-derived exosomes and microvesicles during isolation and detection. Scientific reports. 2016;6:24316.
19. Oksvold MP, Kullmann A, Forfang L, Kierulf B, Li M, Brech A, et al. Expression of B-cell surface antigens in subpopulations of exosomes released from B-cell lymphoma cells. Clinical therapeutics. 2014;36(6):847-62. e1.
20. Jella K, Nasti T, Li Z, Malla S, Buchwald Z, Khan M. Exosomes, their biogenesis and role in inter-cellular communication, tumor microenvironment and cancer immunotherapy. Vaccines. 2018;6(4):69.
21. Meehan K, Vella LJ. The contribution of tumour-derived exosomes to the hallmarks of cancer. Critical reviews in clinical laboratory sciences. 2016;53(2):121-31.
22. Miller IV, Grunewald TG. Tumour-derived exosomes: Tiny envelopes for big stories. Biology of the Cell. 2015;107(9):287-305.
23. Bebelman MP, Smit MJ, Pegtel DM, Baglio SR. Biogenesis and function of extracellular vesicles in cancer. Pharmacology & therapeutics. 2018;188:1-11.
24. Kowal J, Arras G, Colombo M, Jouve M, Morath JP, Primdal-Bengtson B, et al. Proteomic comparison defines novel markers to characterize heterogeneous populations of extracellular vesicle subtypes. 2016:201521230.
25. Rana S, Zöller M. Exosome target cell selection and the importance of exosomal tetraspanins: a hypothesis. Portland Press Limited; 2011.
26. Cocucci E, Meldolesi J. Ectosomes and exosomes: shedding the confusion between extracellular vesicles. Trends in cell biology. 2015;25(6):364-72.
27. Hong C-S, Muller L, Whiteside TL, Boyiadzis M. Plasma exosomes as markers of therapeutic response in patients with acute myeloid leukemia. Frontiers in immunology. 2014;5:160.
28. Boyiadzis M, Whiteside TL. Plasma-derived exosomes in acute myeloid leukemia for detection of minimal residual disease: are we ready? Expert review of molecular diagnostics. 2016;16(6):623-9.
29. Boyiadzis M, Whiteside TL. Information transfer by exosomes: A new frontier in hematologic malignancies. Blood reviews. 2015;29(5):281-90.
30. Patel GK, Khan MA, Zubair H, Srivastava SK, Singh S, Singh AP. Comparative analysis of exosome isolation methods using culture supernatant for optimum yield, purity and downstream applications. Scientific reports. 2019;9(1):1-10.
31. Böing AN, Van Der Pol E, Grootemaat AE, Coumans FA, Sturk A, Nieuwland RJJoev. Single-step isolation of extracellular vesicles by size-exclusion chromatography. 2014;3(1):23430.
32. Namburi S, Broxmeyer HE, Whiteside TL, Boyiadzis M. Plasma-derived exosomes in acute myeloid leukemia carry dipeptidylpeptidase-4 and inhibit normal human hematopoiesis. Am Soc Hematology; 2017.
33. Headland SE, Jones HR, D'sa AS, Perretti M, Norling LV. Cutting-edge analysis of extracellular microparticles using ImageStream X imaging flow cytometry. Scientific reports. 2014;4:5237.
34. Zuba-Surma EK, Kucia M, Abdel-Latif A, Lillard JW, Ratajczak MZ. The ImageStream System: a key step to a new era in imaging. Folia histochemica et cytobiologica. 2007;45(4):279-90.
35. Butt IA. Analysis of ligands for NK cell receptors in cells and exosomes from acute leukemia patients 2016.
36. Guttman O, Baranovski B, Schuster R, Kaner Z, Freixo-Lima G, Bahar N, et al. Acute-phase protein α1-anti-trypsin: diverting injurious innate and adaptive immune

responses from non-authentic threats. Clinical & Experimental Immunology. 2015;179(2):161-72.
37. Sah N, Khan Z, Khan G, Bisen P. Structural, functional and therapeutic biology of survivin. Cancer letters. 2006;244(2):164-71.
38. Butt IA. Analysis of ligands for NK cell receptors in cells and exosomes from acute leukemia patients. Master thesis, University of Oslo. 2016.
39. Baranyai T, Herczeg K, Onódi Z, Voszka I, Módos K, Marton N, et al. Isolation of exosomes from blood plasma: qualitative and quantitative comparison of ultracentrifugation and size exclusion chromatography methods. PloS one. 2015;10(12).
40. Parsons ME, McParland D, Szklanna PB, Guang MHZ, O'Connell K, O'Connor HD, et al. A protocol for improved precision and increased confidence in nanoparticle tracking analysis concentration measurements between 50 and 120 nm in biological fluids. Frontiers in cardiovascular medicine. 2017;4:68.
41. Gardiner C, Ferreira YJ, Dragovic RA, Redman CW, Sargent IL. Extracellular vesicle sizing and enumeration by nanoparticle tracking analysis. Journal of extracellular vesicles. 2013;2(1):19671.
42. Vergauwen G, Dhondt B, Van Deun J, De Smedt E, Berx G, Timmerman E, et al. Confounding factors of ultrafiltration and protein analysis in extracellular vesicle research. Scientific reports. 2017;7(1):1-12.
43. Martins TS, Catita J, Rosa IM, e Silva OAdC, Henriques AG. Exosome isolation from distinct biofluids using precipitation and column-based approaches. PLoS One. 2018;13(6).
44. Helwa I, Cai J, Drewry MD, Zimmerman A, Dinkins MB, Khaled ML, et al. A comparative study of serum exosome isolation using differential ultracentrifugation and three commercial reagents. PloS one. 2017;12(1).
45. Caradec J, Kharmate G, Hosseini-Beheshti E, Adomat H, Gleave M, Guns E. Reproducibility and efficiency of serum-derived exosome extraction methods. Clinical biochemistry. 2014;47(13-14):1286-92.
46. Saunderson SC, Schuberth PC, Dunn AC, Miller L, Hock BD, MacKay PA, et al. Induction of exosome release in primary B cells stimulated via CD40 and the IL-4 receptor. The Journal of Immunology. 2008;180(12):8146-52.
47. Yakimchuk K. Exosomes: isolation and characterization methods and specific markers. Mater Methods. 2015;5:1450-3.
48. Szczepanski MJ, Szajnik M, Welsh A, Whiteside TL, Boyiadzis M. Blast-derived microvesicles in sera from patients with acute myeloid leukemia suppress natural killer cell function via membrane-associated transforming growth factor-β1. Haematologica. 2011;96(9):1302-9.
49. Tarze A, Deniaud A, Le Bras M, Maillier E, Mollé D, Larochette N, et al. GAPDH, a novel regulator of the pro-apoptotic mitochondrial membrane permeabilization. Oncogene. 2007;26(18):2606-20.
50. Tisdale EJ, Azizi F, Artalejo CR. Rab2 utilizes glyceraldehyde-3-phosphate dehydrogenase and protein kinase Cι to associate with microtubules and to recruit dynein. Journal of Biological Chemistry. 2009;284(9):5876-84.
51. Dar GH, Mendes CC, Kuan W-L, Conceição M, El-Andaloussi S, Mager I, et al. GAPDH controls extracellular vesicle biogenesis and enhances therapeutic potential of EVs in silencing the Huntingtin gene in mice via siRNA delivery. bioRxiv. 2020.
52. Rao VN, Reddy E. elk-1 proteins interact with MAP kinases. Oncogene. 1994;9(7):1855-60.
53. van der Mijn JC, Sol N, Mellema W, Jimenez CR, Piersma SR, Dekker H, et al. Analysis of AKT and ERK1/2 protein kinases in extracellular vesicles isolated from blood of patients with cancer. Journal of extracellular vesicles. 2014;3(1):25657.

54. Svensson KJ, Christianson HC, Wittrup A, Bourseau-Guilmain E, Lindqvist E, Svensson LM, et al. Exosome uptake depends on ERK1/2-heat shock protein 27 signaling and lipid Raft-mediated endocytosis negatively regulated by caveolin-1. Journal of Biological Chemistry. 2013;288(24):17713-24.
55. Feingold KR, Grunfeld C. Introduction to lipids and lipoproteins. Endotext [Internet]: MDText. com, Inc.; 2018.
56. McNeish I, Bell S, McKay T, Tenev T, Marani M, Lemoine N. Expression of Smac/DIABLO in ovarian carcinoma cells induces apoptosis via a caspase-9-mediated pathway. Experimental cell research. 2003;286(2):186-98.
57. Ibrahim A, Zahran AM, Aly SS, Refaat A, Hassan MH. CD56 and CD11b Positivity with Low Smac/DIABLO Expression as Predictors of Chemoresistance in Acute Myeloid Leukaemia: Flow Cytometric Analysis. Asian Pacific journal of cancer prevention: APJCP. 2018;19(11):3187.
58. Moldovan G-L, Pfander B, Jentsch S. PCNA, the maestro of the replication fork. Cell. 2007;129(4):665-79.
59. Shemesh A, Kundu K, Peleg R, Yossef R, Kaplanov I, Ghosh S, et al. NKp44-derived peptide binds proliferating cell nuclear antigen and mediates tumor cell death. Frontiers in immunology. 2018;9:1114.
60. Mathew P, Horton N, Bowen K, Mathew S. Lectin-like transcript-1 (LLT1) and exosomal PCNA inhibit NK cell effector function against prostate cancer cells (TUM2P. 892). Am Assoc Immnol; 2014.
61. Gettins PG. Serpin structure, mechanism, and function. Chemical reviews. 2002;102(12):4751-804.
62. Kreger BT, Johansen ER, Cerione RA, Antonyak MA. The enrichment of survivin in exosomes from breast cancer cells treated with paclitaxel promotes cell survival and chemoresistance. Cancers. 2016;8(12):111.
63. Nawaz M, Camussi G, Valadi H, Nazarenko I, Ekström K, Wang X, et al. The emerging role of extracellular vesicles as biomarkers for urogenital cancers. Nature Reviews Urology. 2014;11(12):688.
64. Levesque J-P, Winkler IG. Cell adhesion molecules in normal and malignant hematopoiesis: from bench to bedside. Current Stem Cell Reports. 2016;2(4):356-67.
65. Pap E, Pallinger E, Falus A, Kiss A, Kittel A, Kovacs P, et al. T lymphocytes are targets for platelet-and trophoblast-derived microvesicles during pregnancy. Placenta. 2008;29(9):826-32.
66. Tinoco R, Carrette F, Barraza ML, Otero DC, Magaña J, Bosenberg MW, et al. PSGL-1 is an immune checkpoint regulator that promotes T cell exhaustion. Immunity. 2016;44(5):1190-203.

APPENDIX 1: ABBREVIATIONS

ALL	Acute lymphoid leukemia
AML	Acute myeloid leukemia
B-ALL	B-cell acute lymphoid leukemia
BCP	B-cell Precursor
CD	Cluster of differentiation
Ch	Channel
CFDA-SE	Carboxyfluorescein diacetate succinimidyl ester
CFSE	Carboxyfluorescein succiminidyl ester
CLL	Chronic lymphoid leukemia
CML	Chronic myeloid leukemia
dH_2O	Distilled water
ERK	Extracellular signal-regulated kinase
ESCRT	Endosomal sorting complex required for transport
EVs	Extracellular vesicles
fPBS	Filtered PBS
FTLA	Finite track length adjustment
HDL	High density lipoprotein
IDL	Intermediate density lipoprotein
ISx	Image Stream
LAA	Leukemic associated antigens
MAP	Mitogen Activated Protein
MHC	Major histocompatibility complex
MRD	Minimal residual disease
mRNA	Messenger RNA
miRNA	Micro RNA
MVB	Multivesicular bodies
MVs	Microvesicles
NK cells	Natural Killer cells
NOPHO	Nordic Society of Pediatric Hematology and Oncology
NTA	Nanoparticle tracking analysis

OUH	Oslo University Hospital
PBS	Phosphate buffer saline
PM	Plasma membrane
PVDF	Polyvinylidene difluoride
RNA	Ribonucleic acid
SUDHL-6	Stanford university-diffuse histiocytic lymphoma-6
SCT	Stem cell transplantation
SDS – PAGE	Sodium dodecyl sulfate polyacrylamide gel electrophoresis
SEC	Size-exclusion chromatography
sEV	Small extracellular vesicle
T-ALL	T-cell acute lymphoid leukemia
TBS	Tris buffered saline
TBS-T	Tris buffered saline - Tween
TEM	Transmission electron microscopy
VLDL	Very low-density lipoprotein
WBC	White blood cells

APPENDIX 2: PATIENTS AND CONTROLS

Controls	Age	Patients	Age	Disease	Risk group	WBC at diagnosis (x10^9/mL)
C05	7	P55	5	BCP-ALL	SR	19,7
C08	3	P56	5	BCP-ALL	SR	15,8
C09	4	P61	1	BCP-ALL	SR	22,0
C22	16	P62	1	BCP-ALL	SR	5,9
C23	15	P64	6	BCP-ALL	SR	1,9
C24	5	P66	16	BCP-ALL	SR	7,2
C27	15	P74	15	BCP-ALL	IR	1,1
C32	1	P71	13	T-ALL	HR	7,2
C35	5	P57	8	AML	HR	15,9
C39	5	P67	1	AML	SR	13,2
		P69	1	AML	SR	4,3
		P72	2	AML	SR	6,2

APPENDIX 3: BUFFERS AND SOLUTIONS

2x SDS lysis buffer

Triton X-100 (10 %), 200 µl

NaCl/Tris, 750 µl

Protease inhibitor cocktail, 20 µl

10 x PBS

NaCl (1.37 M), 80 g

KCl (27 mM), 2 g

Na_2HPO_4- ·2 H_2O (43 mM), 7.7 g

KH_2PO_4 (14 mM), 2 g

H_2O, 1L

1 x PBS, pH 7.4

10 x PBS, 100 ml

ddH_2O, 900 ml

pH adjusted to 7.4

PBS-Tween

25 x PBS, 40 ml

ddH_2O, 960 ml

Tween20, 10 ml

PBS-Tween + 5 % BSA

PBS-Tween (see above), 100 ml

BSA, 5 g

1x SDS running buffer 1L

10 x running buffer, 100 ml

dH_2O, 900 ml

4 x SDS Loading buffer

80% glycerol, 5 ml

1M Tris-HCl, pH 6.8, 2.4 ml

SDS, 0.8 g

Bromophenol blue, 4 mg

dH_2O, 2.1 ml

10x SDS running buffer pH 8.3

Tris base, 30 g

Glycine, 144 g

SDS, 10 g

dH_2O to 1 L

10 x TBS (tris-buffered saline) buffer

Tris-Cl (1M, pH 7.5), 24 g

NaCl (1.5 M), 88 g

Tris base, 56 g

dH_2O, 900 ml

TBS-Tween

10 x TBS, 100 ml

dH_2O, 900 ml

Tween-20, 500µl

Blocking buffer (5 % skimmed milk)

Skimmed dry milk, 2.5 g

TBS-T, 50 ml

Transfer buffer, western using PVDF membrane

Glycine, 28.8 g

Tris-base, 6.04 g

Methanol, 200 µl

ddH_2O, 1.6 L

PBS + Citrate 0.32%

1x PBS, 100 ml

Citric acid, 0.32 g

Urea elution buffer:

Urea, 24 g

dH_2O, 45 ml

Dissolve urea before adding 5 ml 1 M Tris/10% Triton X-100

Bead block buffer

50 ml blocking buffer w/Casein (ThermoFisher Scientific, Waltham, MA)

100 µl goat, rabbit, mouse IgGs (Jackson Immunolabs)

50 µl human IgG (Jackson Immunolabs)

APPENDIX 4: ANTIBODIES

Appendix table 4.1: Overview of antibodies used for Image Stream

Name	Conjugate	Clone	Conc/test	Producer
CD63	PE	H5C6	5µg	ThermoFisher

Appendix table 4.2: Overview of antibodies used for western blotting

Name	Clone	Host	Isotype	Dilutions	Producer
CD63	TS63	Mouse	IgG1	1:500	ThermoFisher
CD81	M38	Mouse	IgG1	1:500	ThermoFisher
CD19	Polyclonal	Rabbit	IgG	1:100	Novus Biologicals
CD34	Monoclonal	Rabbit	IgG	1:100	Novus Biologicals
Survivin	9H18L32	Rabbit	IgG	1:500	ThermoFisher
PSGL-1	68810	Mouse	IgG2a	1:100	Novus Biologicals
a_1-antitrypsin	Polyclonal	Goat	IgG	1:100	R&D Systems
Goat Anti-Mouse IgG(H+L)-HRP Conjugate				1:5000	Bio-Rad
Goat Anti-Rabbit IgG(H+L)-HRP Conjugate				1:5000	Bio-Rad
Rabbit Anti-Goat IgG(H+L)-HRP Conjugate				1:5000	ThermoFisher